

Decentralized Quantized Kalman Filtering With Scalable Communication Cost

Eric J. Msechu, *Student Member, IEEE*, Stergios I. Roumeliotis, *Member, IEEE*, Alejandro Ribeiro, *Member, IEEE*,
and Georgios B. Giannakis, *Fellow, IEEE*

Abstract—Estimation and tracking of generally nonstationary Markov processes is of paramount importance for applications such as localization and navigation. In this context, *ad hoc* wireless sensor networks (WSNs) offer decentralized Kalman filtering (KF) based algorithms with documented merits over centralized alternatives. Adhering to the limited power and bandwidth resources WSNs must operate with, this paper introduces two novel decentralized KF estimators based on quantized measurement innovations. In the first quantization approach, the region of an observation is partitioned into N contiguous, nonoverlapping intervals where each partition is binary encoded using a block of m bits. Analysis and Monte Carlo simulations reveal that with minimal communication overhead, the mean-square error (MSE) of a novel decentralized KF tracker based on 2-3 bits comes stunningly close to that of the clairvoyant KF. In the second quantization approach, if intersensor communications can afford m bits at time n , then the i th bit is iteratively formed using the sign of the difference between the n th observation and its estimate based on past observations (up to time $n - 1$) along with previous bits (up to $i - 1$) of the current observation. Analysis and simulations show that KF-like tracking based on m bits of iteratively quantized innovations communicated among sensors exhibits MSE performance identical to a KF based on analog-amplitude observations applied to an observation model with noise variance increased by a factor of $[1 - (1 - 2/\pi)^m]^{-1}$.

Index Terms—Decentralized state estimation, Kalman filtering, limited-rate communication, quantized observations, target tracking, wireless sensor networks.

I. INTRODUCTION

CONSIDER an *ad-hoc* wireless sensor network (WSN) deployed to track a Markov stochastic process. Each sensor node acquires observations which are noisy linear transformations of a common state. The sensors then transmit

Manuscript received August 12, 2007; revised April 14, 2008. The associate editor coordinating the review of this manuscript and approving it for publication was Dr. Hongbin Li. Prepared through collaborative participation in the Communication and Networks Consortium sponsored by the U. S. Army Research Lab under the Collaborative Technology Alliance Program, Cooperative Agreement DAAD19-01-2-0011. The U.S. Government is authorized to reproduce and distribute reprints for Government purposes notwithstanding any copyright notation thereon. Parts of this work were presented at the Asilomar Conference of Signals, Systems, and Computers, Pacific Grove, CA, November 2007, and at the IEEE Conference on Acoustics, Speech and Signal Processing, Las Vegas, NV, April 2008.

E. J. Msechu, A. Ribeiro, and G. B. Giannakis are with the Department of Electrical and Computer Engineering, University of Minnesota, Minneapolis, MN 55455 USA (e-mail: emsechu@ece.umn.edu; aribeiro@ece.umn.edu; georgios@ece.umn.edu).

S. I. Roumeliotis is with the Department of Computer Science and Engineering, University of Minnesota, Minneapolis, MN 55455 USA (e-mail: stergioscs.umn.edu).

Color versions of one or more of the figures in this paper are available online at <http://ieeexplore.ieee.org>.

Digital Object Identifier 10.1109/TSP.2008.925931

observations to each other in order to form a state estimate. If observations were available at a common location, minimum mean-square error (MMSE) estimates could be obtained using a Kalman filter (KF). However, since observations are distributed in space and there is limited communication bandwidth, the observations have to be quantized before transmission. Thus, the original estimation problem is transformed into decentralized state estimation based on quantized observations. The problem is further complicated by the harsh environment typical of WSNs; see e.g., [3] and [4].

Quantizing observations to estimate a parameter of interest, is *not* the same as quantizing a signal for later reconstruction [7]. Instead of a reconstruction algorithm, the objective is finding, e.g., MMSE optimal, estimators using quantized observations [19], [20]. Furthermore, optimal quantizers for reconstruction are, generally, different from optimal quantizers for estimation.

State estimation using quantized observations is a nonlinear estimation problem that can be solved using e.g., unscented (U)KFs [11] or particle filters [5]. Surprisingly, for the case where quantized observations are defined as the sign of the innovation (SoI) sequence, it is possible to derive a filter with complexity and performance very close to the clairvoyant KF based on the analog-amplitude observations [21]. Even though promising, the approach of [21] is limited to a particular 1-bit per observation quantizer.

This paper builds on and considerably broadens the scope of [21] by addressing the middle ground between estimators based on severely quantized (1-bit) data and those based on un-quantized data. The end result is quantizer-estimator structures that offer desirable trade-offs between bandwidth requirements (dictating the number of quantization bits used for intersensor communications) and overall tracking performance (assessed by the mean-square state estimation error).

The rest of the paper is organized as follows. Problem statement including the modeling assumptions are in Section II. Section III presents a quantizer-estimator based on multi-level batch quantization, whereas Section IV describes a second quantizer-estimator that relies on iterative multi-bit quantization. (For a high-level description of the batch and iterative approaches, see also Fig. 1.) Performance analysis of the iterative quantizer-estimator is also detailed in Section IV. Simulations in Section V are used to corroborate the analytical discourse and compare the two quantization approaches.

Notation: Vectors (resp. matrices) are denoted using lower (upper) case bold face letters. The probability density function (pdf) of x conditioned on y is represented by $p(x|y)$, where x denotes the random variable as well as the value it takes. The Gaussian pdf with mean $E\{\mathbf{x}\} = \boldsymbol{\mu}$ and covariance matrix $\text{cov}\{\mathbf{x}\} = \mathbf{C}$ is represented as $p(\mathbf{x}) = \mathcal{N}[\mathbf{x}; \boldsymbol{\mu}, \mathbf{C}]$ and $Q(z) := \int_z^\infty \mathcal{N}[x; 0, 1] dx$. The probability mass function for a discrete random variable b is denoted as $\Pr\{b\}$. Estimators

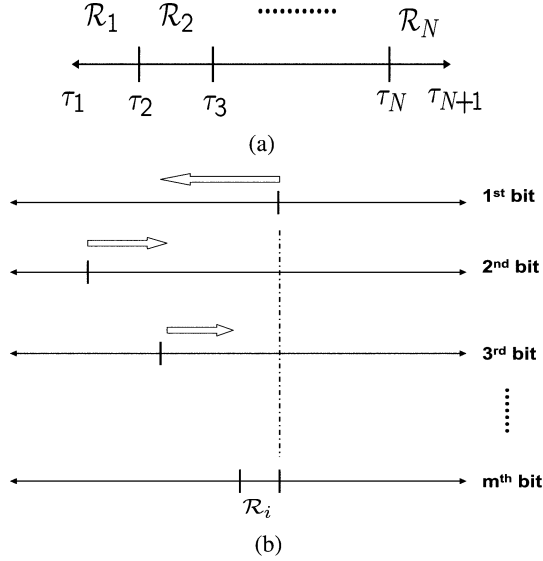


Fig. 1. (a) Batch quantization: $\log_2 N$ bits are generated in a single step to index each of the N regions \mathcal{R}_i where an observation could lie. (b) Iterative quantization: m bits are generated in m steps (iterations).

(or estimates) will be represented using a hat, e.g., $\hat{\mathbf{x}}(n | \mathbf{w}_{1:m})$, where discrete-time indexes should be read as $\hat{\mathbf{x}}(n | \mathbf{w}_{1:m}) := E\{\mathbf{x}(n) | w(1), \dots, w(m)\}$. Finally, T will stand for transposition and δ_{ij} (respectively $\delta(t)$) for the Kronecker (Dirac) delta function.

II. MODELS AND PROBLEM STATEMENT

Consider an ad hoc WSN whose K sensor nodes $\{\mathcal{S}_k\}_{k=1}^K$ are deployed to estimate a multivariate discrete-time random process $\mathbf{x}(n) \in \mathbb{R}^p$. The state equation is given as

$$\mathbf{x}(n) = \mathbf{A}(n) \mathbf{x}(n-1) + \mathbf{u}(n) \quad (1)$$

where $\mathbf{A}(n) \in \mathbb{R}^{p \times p}$ denotes the state transition matrix and $\mathbf{u}(n)$ the driving noise, assumed to be a zero-mean white Gaussian process with covariance matrix $E\{\mathbf{u}(n) \mathbf{u}^T(m)\} = \mathbf{C}_u(n) \delta_{nm}$.

Each sensor records scalar observations $y_k(n)$ adhering to a linear measurement equation

$$y_k(n) = \mathbf{h}_k^T(n) \mathbf{x}(n) + v_k(n) \quad (2)$$

where k is the sensor index, $\mathbf{h}_k(n) \in \mathbb{R}^p$ denotes the regression vector, and $v_k(n)$ is a temporally and spatially white zero-mean Gaussian noise process with covariance $E\{v_k(n) v_l(m)\} = c_v(n) \delta_{nm} \delta_{kl}$. It is further assumed that $\mathbf{u}(n)$ is independent of both $v_k(n)$ and $\mathbf{x}(0)$.

Supposing that $\mathbf{A}(n)$, $\mathbf{C}_u(n)$, $\mathbf{h}_k(n)$ and $c_v(n)$ are available $\forall n, k$ from the physical model of the problem, the goal of the WSN is for each sensor to form an estimate of $\mathbf{x}(n)$ to be used, e.g., in a habitat monitoring [15], or as a first step in a distributed control setup [10]. Estimating $\mathbf{x}(n)$ necessitates each sensor \mathcal{S}_k to communicate $y_k(n)$ to all other sensors $\{\mathcal{S}_l\}_{l=1, l \neq k}^K$. Communication takes place over the shared wireless channel that we assume can afford transmission of a single packet of m bits per time slot n . This leads to a one-to-one correspondence between time n and sensor index k and allows us to drop the sensor argument k in (2).

Each sensor in the network does both data gathering (sensing) and signal processing (estimation from broadcast data and local observations). The collection of cooperating sensor nodes forms

an *ad hoc* network without a central fusion unit. Thus, signal processing at each node based on data exchanged among sensors as well as local observations constitutes the decentralized filtering at hand.

The decision as to which sensor $\mathcal{S}_k = \mathcal{S}(n)$ broadcasts at time n , and consequently which observation $y_k(n) = y(n)$ is transmitted, depends on the underlying scheduling algorithm. Time-division multiple-access is assumed and for simplicity each sensor's broadcast footprint reaches the entire collaborating set of sensors. More elaborate sensor scheduling techniques—see e.g., [8], [18] and references therein—can be considered but are beyond the scope of this paper.

A. MMSE Estimation With Quantized Observations

In order to effect digital intersensor communication in the bandwidth-limited WSN, the observations $y(n) \in \mathbb{R}$ are quantized. With \mathcal{B} denoting a finite set of quantization messages¹, we investigate quantization rules $\mathbf{q}_n[\cdot]$ of the form

$$b(n) := \mathbf{q}_n[y(n)], \quad \text{where } \mathbf{q}_n : \mathbb{R} \rightarrow \mathcal{B}. \quad (3)$$

Given current and past messages $\mathbf{b}_{1:n} := \{b(1), b(2), \dots, b(n)\}$, we are interested in developing estimates $\hat{\mathbf{x}}(n | \mathbf{b}_{1:n})$ of the state $\mathbf{x}(n)$. The error covariance matrix (ECM) of the estimator is defined as $\mathbf{M}(n | \mathbf{b}_{1:n}) := E\{\hat{\mathbf{x}}(n | \mathbf{b}_{1:n}) - \mathbf{x}(n) [\hat{\mathbf{x}}(n | \mathbf{b}_{1:n}) - \mathbf{x}(n)]^T\}$, and the mean-square error (MSE) of $\hat{\mathbf{x}}(n | \mathbf{b}_{1:n})$ is given by the trace of the ECM, i.e., $\text{tr}\{\mathbf{M}(n | \mathbf{b}_{1:n})\}$. As is well known, see e.g., [17, Ch. 5], the desired MMSE estimator is given by the conditional mean

$$\hat{\mathbf{x}}(n | \mathbf{b}_{1:n}) := E\{\mathbf{x}(n) | \mathbf{b}_{1:n}\} = \int_{\mathbb{R}^p} \mathbf{x}(n) p[\mathbf{x}(n) | \mathbf{b}_{1:n}] d\mathbf{x}(n). \quad (4)$$

To obtain a closed-form expression for $\hat{\mathbf{x}}(n | \mathbf{b}_{1:n})$, the posterior distribution $p[\mathbf{x}(n) | \mathbf{b}_{1:n}]$ has to be known and the integral in (4) needs to be computable. In principle, $p[\mathbf{x}(n) | \mathbf{b}_{1:n}]$ can be obtained from the state-observation model in (1)–(2) using the prediction-correction steps [P1]–[C1] outlined next.

[P1] Prediction step. With $p[\mathbf{x}(n-1) | \mathbf{b}_{1:n-1}]$ known, the prior pdf, at time index n , $p[\mathbf{x}(n) | \mathbf{b}_{1:n-1}]$ follows from the theorem of total probability

$$p[\mathbf{x}(n) | \mathbf{b}_{1:n-1}] = \int_{\mathbb{R}^p} p[\mathbf{x}(n) | \mathbf{x}(n-1), \mathbf{b}_{1:n-1}] \times p[\mathbf{x}(n-1) | \mathbf{b}_{1:n-1}] d\mathbf{x}(n-1). \quad (5)$$

Note that conditioning on $\mathbf{x}(n-1)$ in $p[\mathbf{x}(n) | \mathbf{x}(n-1), \mathbf{b}_{1:n-1}]$, renders conditioning on $\mathbf{b}_{1:n-1}$ redundant [cf. (1)]; consequently $p[\mathbf{x}(n) | \mathbf{x}(n-1), \mathbf{b}_{1:n-1}] = p[\mathbf{x}(n) | \mathbf{x}(n-1)] = \mathcal{N}[\mathbf{x}(n); \mathbf{A}(n)\mathbf{x}(n-1), \mathbf{C}_u(n)]$. The pdf $p[\mathbf{x}(n) | \mathbf{b}_{1:n-1}]$ can be used to predict the state $\mathbf{x}(n)$ using past messages $\mathbf{b}_{1:n-1}$ and the state evolution model (1).

[C1] Correction step. When new observations become available, we write $p[\mathbf{x}(n) | \mathbf{b}_{1:n}] = p[\mathbf{x}(n) | \mathbf{b}_{1:n-1}, b(n)]$ using Bayes' rule as

$$p[\mathbf{x}(n) | \mathbf{b}_{1:n}] = p[\mathbf{x}(n) | \mathbf{b}_{1:n-1}] \frac{\Pr\{b(n) | \mathbf{x}(n), \mathbf{b}_{1:n-1}\}}{\Pr\{b(n) | \mathbf{b}_{1:n-1}\}} \quad (6)$$

where the probability $\Pr\{b(n) | \mathbf{x}(n), \mathbf{b}_{1:n-1}\}$ can be obtained using the quantization rule $\mathbf{q}_n[y(n)]$ in (3).

¹These messages are represented by the set $\{1, 2, \dots, |\mathcal{B}|\}$, where each quantization message, i.e., binary codeword $b(n) \in \mathcal{B}$, can be represented by $\log_2 |\mathcal{B}|$ bits.

Likewise, $\Pr\{b(n) | \mathbf{b}_{1:n-1}\}$ depends on $\mathbf{q}_n[y(n)]$ and the prediction pdf $p[\mathbf{x}(n) | \mathbf{b}_{1:n-1}]$; in Sections III and IV specific quantizer structures and resulting pdfs are explored.

The Kalman filter (KF) is a recursive algorithm of the form [P1]-[C1]. In our framework KF corresponds to the transmission of un-quantized messages $b(n) = y(n)$, i.e., a clairvoyant scenario without bandwidth constraints. In this case, the pdfs in (5) and (6) are Gaussian and it suffices to propagate their means and covariance matrices leading to the Kalman recursions [P2]-[C2].

[P2] Prediction step. Consider the predicted estimate $\hat{\mathbf{x}}(n | \mathbf{y}_{1:n-1}) := E\{\mathbf{x}(n) | \mathbf{y}_{1:n-1}\}$ and let $\mathbf{M}(n | \mathbf{y}_{1:n-1}) := E\{[\hat{\mathbf{x}}(n | \mathbf{y}_{1:n-1}) - \mathbf{x}(n)][\hat{\mathbf{x}}(n | \mathbf{y}_{1:n-1}) - \mathbf{x}(n)]^T\}$ denote the corresponding ECM. Given the previous estimate $\hat{\mathbf{x}}(n-1 | \mathbf{y}_{1:n-1})$ and its ECM $\mathbf{M}(n-1 | \mathbf{y}_{1:n-1})$, we have

$$\hat{\mathbf{x}}(n | \mathbf{y}_{1:n-1}) = \mathbf{A}(n)\hat{\mathbf{x}}(n-1 | \mathbf{y}_{1:n-1}) \quad (7)$$

$$\mathbf{M}(n | \mathbf{y}_{1:n-1}) = \mathbf{A}(n)\mathbf{M}(n-1 | \mathbf{y}_{1:n-1})\mathbf{A}^T(n) + \mathbf{C}_u(n). \quad (8)$$

[C2] KF correction step. Consider the predicted data $\hat{y}(n | \mathbf{y}_{1:n-1}) := E\{y(n) | \mathbf{y}_{1:n-1}\} = \mathbf{h}^T(n)\hat{\mathbf{x}}(n | \mathbf{y}_{1:n-1})$ and their innovation $\tilde{y}(n | \mathbf{y}_{1:n-1}) := y(n) - \hat{y}(n | \mathbf{y}_{1:n-1})$. Then $\hat{\mathbf{x}}(n | \mathbf{y}_{1:n})$ in (4) and its ECM obey

$$\begin{aligned} \hat{\mathbf{x}}(n | \mathbf{y}_{1:n}) &= \hat{\mathbf{x}}(n | \mathbf{y}_{1:n-1}) \\ &+ \frac{\mathbf{M}(n | \mathbf{y}_{1:n-1})\mathbf{h}(n)}{\mathbf{h}^T(n)\mathbf{M}(n | \mathbf{y}_{1:n-1})\mathbf{h}(n) + c_v(n)} \tilde{y}(n | \mathbf{y}_{1:n-1}) \end{aligned} \quad (9)$$

$$\begin{aligned} \mathbf{M}(n | \mathbf{y}_{1:n}) &= \mathbf{M}(n | \mathbf{y}_{1:n-1}) \\ &- \frac{\mathbf{M}(n | \mathbf{y}_{1:n-1})\mathbf{h}(n)\mathbf{h}^T(n)\mathbf{M}(n | \mathbf{y}_{1:n-1})}{\mathbf{h}^T(n)\mathbf{M}(n | \mathbf{y}_{1:n-1})\mathbf{h}(n) + c_v(n)}. \end{aligned} \quad (10)$$

Computations for the KF iterations in [P2]-[C2] are simpler than for the general iteration [P1]-[C1] with quantized observations. Indeed, while [P2]-[C2] requires a few algebraic operations per time-step n , [P1]-[C1] requires: i) numerical integration to obtain the prediction pdf $p[\mathbf{x}(n) | \mathbf{b}_{1:n-1}]$ in (5); ii) numerical update of the posterior pdf $p[\mathbf{x}(n) | \mathbf{b}_{1:n}]$ using Bayes' rule in (6); and iii) numerical integration to evaluate the expectation in (4) and obtain $\hat{\mathbf{x}}(n | \mathbf{b}_{1:n})$.

This high computational cost is inherent to nonlinear models thus motivating approximate filters e.g., the extended (E)KF, the unscented (U)KF, and the particle filter (PF). (Nonlinearity in this paper is due to quantization of the observations.) An alternative workaround is by Gaussian approximation of the prior pdf $p[\mathbf{x}(n) | \mathbf{b}_{1:n-1}]$, see e.g., [13]. This simplifies coping with the potentially intractable pdf $p[\mathbf{x}(n) | \mathbf{b}_{1:n-1}]$ by tracking its mean and covariance matrix which results in the following iteration [P3]-[C3]:

[P3] Prediction step. Define the predicted estimate $\hat{\mathbf{x}}(n | \mathbf{b}_{1:n-1}) := E\{\mathbf{x}(n) | \mathbf{b}_{1:n-1}\}$ and the corresponding ECM $\mathbf{M}(n | \mathbf{b}_{1:n-1}) := E\{[\hat{\mathbf{x}}(n | \mathbf{b}_{1:n-1}) - \mathbf{x}(n)][\hat{\mathbf{x}}(n | \mathbf{b}_{1:n-1}) - \mathbf{x}(n)]^T\}$. Given the previous estimate $\hat{\mathbf{x}}(n-1 | \mathbf{b}_{1:n-1})$ and its ECM $\mathbf{M}(n-1 | \mathbf{b}_{1:n-1})$, linearity of the expectation operator yields

$$\hat{\mathbf{x}}(n | \mathbf{b}_{1:n-1}) = \mathbf{A}(n)\hat{\mathbf{x}}(n-1 | \mathbf{b}_{1:n-1}) \quad (11)$$

$$\mathbf{M}(n | \mathbf{b}_{1:n-1}) = \mathbf{A}(n)\mathbf{M}(n-1 | \mathbf{b}_{1:n-1})\mathbf{A}^T(n) + \mathbf{C}_u(n). \quad (12)$$

[C3] Correction step. Adopt the approximation $p[\mathbf{x}(n) | \mathbf{b}_{1:n-1}] = \mathcal{N}[\mathbf{x}(n); \hat{\mathbf{x}}(n | \mathbf{b}_{1:n-1}), \mathbf{M}(n | \mathbf{b}_{1:n-1})]$. As in [C1], write $p[\mathbf{x}(n) | \mathbf{b}_{1:n}] = p[\mathbf{x}(n) | \mathbf{b}_{1:n-1}, b(n)]$ and use Bayes' rule to obtain

$$\begin{aligned} p[\mathbf{x}(n) | \mathbf{b}_{1:n}] &= \mathcal{N}[\mathbf{x}(n); \hat{\mathbf{x}}(n | \mathbf{b}_{1:n-1}), \mathbf{M}(n | \mathbf{b}_{1:n-1})] \\ &\times \frac{\Pr\{b(n) | \mathbf{x}(n), \mathbf{b}_{1:n-1}\}}{\Pr\{b(n) | \mathbf{b}_{1:n-1}\}}. \end{aligned} \quad (13)$$

Numerator and denominator of the second term in (13) can be found using the approximate prior pdf $p[\mathbf{x}(n) | \mathbf{b}_{1:n-1}] = \mathcal{N}[\mathbf{x}(n); \hat{\mathbf{x}}(n | \mathbf{b}_{1:n-1}), \mathbf{M}(n | \mathbf{b}_{1:n-1})]$ —see [21, Remark 3] for justification of the Gaussian approximation. Estimator $\hat{\mathbf{x}}(n | \mathbf{b}_{1:n})$ is then obtained by evaluating the integral in (4).

The computational cost incurred by [P3]-[C3] is between that of [P1]-[C1] and [P2]-[C2]. To obtain $\hat{\mathbf{x}}(n | \mathbf{b}_{1:n})$ using [P3]-[C3] we do not need to evaluate the integral in (5) but we still need to apply Bayes' rule in (13) and evaluate the integral in (4). The KF iteration [P2]-[C2] on the other hand, evaluates the exact MMSE with small computational cost. For our purposes it represents a clairvoyant benchmark in terms of MSE performance and computational cost.

In this paper, batch (Section III) and iterative (Section IV) joint quantization-estimation approaches are pursued. In each case our objectives are: i) to show that the approximate MMSE estimation [P3]-[C3] can be further simplified yielding a filter with comparable computational cost to the KF; and ii) to compare the MSE of [P3]-[C3] using quantized observations, with the MSE of the KF in [P2]-[C2]. We will further contend that the MSE penalty associated with state estimates based on quantized data is small even with coarse quantization down to a few bits per observation.

III. KALMAN FILTERING WITH BATCH QUANTIZED OBSERVATIONS

In this section, each observation $y(n)$ is quantized by partitioning the observation space \mathbb{R} into N intervals $\mathcal{R}_i := [\tau_i(n), \tau_{i+1}(n))$, where $i \in \mathcal{B} := \{1, \dots, N\}$. The quantizer $\mathbf{q}[\cdot]$ is thus specified through the thresholds $\{\tau_i(n)\}_{i=1}^{N+1}$, where $\tau_1(n) = -\infty$, $\tau_i(n) < \tau_{i+1}(n)$, and $\tau_{N+1}(n) = +\infty$. Consider the estimate $\hat{y}(n | \mathbf{b}_{1:n-1}) = E\{y(n) | \mathbf{b}_{1:n-1}\}$, the corresponding innovation sequence $\tilde{y}(n | \mathbf{b}_{1:n-1}) := y(n) - \hat{y}(n | \mathbf{b}_{1:n-1})$, and the quantization rule

$$b(n) = i, \quad \text{iff } \tilde{y}(n | \mathbf{b}_{1:n-1}) \in [\tau_i(n), \tau_{i+1}(n)). \quad (14)$$

In order to compute $\hat{\mathbf{x}}(n | \mathbf{b}_{1:n})$ [cf. (4)], the pdf $p[\mathbf{x}(n) | \mathbf{b}_{1:n}]$ is needed. From (13), the distributions $\Pr\{b(n) = i | \mathbf{b}_{1:n-1}\}$ and $\Pr\{b(n) = i | \mathbf{x}(n), \mathbf{b}_{1:n-1}\}$ characterized in the following equations, need to be known. Using the quantization rule in (14) the events $\{b(n) = i\}$ and $\{\tau_i(n) \leq \tilde{y}(n | \mathbf{b}_{1:n-1}) < \tau_{i+1}(n)\}$ are equivalent and consequently

$$\begin{aligned} \Pr\{b(n) = i | \mathbf{x}(n), \mathbf{b}_{1:n-1}\} \\ = \Pr\{\tau_i(n) \leq \tilde{y}(n | \mathbf{b}_{1:n-1}) < \tau_{i+1}(n) | \mathbf{x}(n), \mathbf{b}_{1:n-1}\}. \end{aligned} \quad (15)$$

Given $\{\mathbf{x}(n), \mathbf{b}_{1:n-1}\}$, the innovation $\tilde{y}(n | \mathbf{b}_{1:n-1}) := y(n) - \hat{y}(n | \mathbf{b}_{1:n-1}) = \mathbf{h}^T(n)[\mathbf{x}(n) - \hat{\mathbf{x}}(n | \mathbf{b}_{1:n-1})] + v(n)$ has conditional pdf $p[\tilde{y}(n | \mathbf{b}_{1:n-1}) | \mathbf{x}(n), \mathbf{b}_{1:n-1}] = \mathcal{N}[\tilde{y}(n | \mathbf{b}_{1:n-1}); \mathbf{h}^T(n)\tilde{\mathbf{x}}(n | \mathbf{b}_{1:n-1}), c_v(n)]$, where $\tilde{\mathbf{x}}(n | \mathbf{b}_{1:n-1}) := \mathbf{x}(n) - \hat{\mathbf{x}}(n | \mathbf{b}_{1:n-1})$. Using this pdf we can rewrite (15) in terms of the Gaussian tail function $Q[\cdot]$ as

$$\begin{aligned} & \Pr\{b(n) = i \mid \mathbf{x}(n), \mathbf{b}_{1:n-1}\} \\ &= Q\left(\frac{\tau_i(n) - \mathbf{h}^T(n)\tilde{\mathbf{x}}(n \mid \mathbf{b}_{1:n-1})}{\sqrt{c_v(n)}}\right) \\ & \quad - Q\left(\frac{\tau_{i+1}(n) - \mathbf{h}^T(n)\tilde{\mathbf{x}}(n \mid \mathbf{b}_{1:n-1})}{\sqrt{c_v(n)}}\right). \quad (16) \end{aligned}$$

Likewise, we can write $\Pr\{b(n) = i \mid \mathbf{b}_{1:n-1}\} = \Pr\{\tau_i(n) \leq \tilde{y}(n \mid \mathbf{b}_{1:n-1}) < \tau_{i+1}(n) \mid \mathbf{b}_{1:n-1}\}$ which is identical to (15) except for the conditioning variables. Note that, unlike (15), the conditional pdf $p[\tilde{y}(n \mid \mathbf{b}_{1:n-1}) \mid \mathbf{b}_{1:n-1}]$ is non-Gaussian. It can though be approximated by using a Gaussian prior for $p[\mathbf{x}(n) \mid \mathbf{b}_{1:n-1}]$ as follows.

If $p[\mathbf{x}(n) \mid \mathbf{b}_{1:n-1}] = \mathcal{N}[\mathbf{x}(n); \hat{\mathbf{x}}(n \mid \mathbf{b}_{1:n-1}), \mathbf{M}(n \mid \mathbf{b}_{1:n-1})]$, then the prior pdf $p[y(n) \mid \mathbf{b}_{1:n-1}]$ is also normal with mean $\hat{y}(n \mid \mathbf{b}_{1:n-1})$ and variance $\sigma_y^2(n) := \mathbf{h}^T(n) \times \mathbf{M}(n \mid \mathbf{b}_{1:n-1}) \mathbf{h}(n) + c_v(n)$ [cf. (2)]. Since the innovation is defined as $\tilde{y}(n \mid \mathbf{b}_{1:n-1}) := y(n) - \hat{y}(n \mid \mathbf{b}_{1:n-1})$, we have $p[\tilde{y}(n \mid \mathbf{b}_{1:n-1}) \mid \mathbf{b}_{1:n-1}] = \mathcal{N}[\tilde{y}(n \mid \mathbf{b}_{1:n-1}); 0, \sigma_y^2(n)]$ and we can thus write

$$\begin{aligned} & \Pr\{b(n) = i \mid \mathbf{b}_{1:n-1}\} \\ &= Q[\tau_i(n)/\sigma_y(n)] - Q[\tau_{i+1}(n)/\sigma_y(n)] \\ &= Q[\Delta_i(n)] - Q[\Delta_{i+1}(n)] \quad (17) \end{aligned}$$

where $\Delta_i(n) := \tau_i(n)/\sigma_y(n)$ are thresholds normalized by the standard deviation of the observations.

Substituting (16) and (17) into (13) we obtain an expression for $p[\mathbf{x}(n) \mid \mathbf{b}_{1:n}]$ that can be used in (4) to obtain $\hat{\mathbf{x}}(n \mid \mathbf{b}_{1:n})$. It is remarkable that with the Gaussian assumption for $p[\mathbf{x}(n) \mid \mathbf{b}_{1:n-1}]$, (4) can be found analytically as summarized in the next proposition.

Proposition 1: Consider the state space model (1)–(2) and quantized observations $b(n)$ defined as in (14). Suppose that the predicted estimate $\hat{\mathbf{x}}(n \mid \mathbf{b}_{1:n-1})$ and corresponding ECM $\mathbf{M}(n \mid \mathbf{b}_{1:n-1})$ are given. If the prediction pdf is $p[\mathbf{x}(n) \mid \mathbf{b}_{1:n-1}] = \mathcal{N}[\mathbf{x}(n); \hat{\mathbf{x}}(n \mid \mathbf{b}_{1:n-1}), \mathbf{M}(n \mid \mathbf{b}_{1:n-1})]$, the MMSE estimator $\hat{\mathbf{x}}(n \mid \mathbf{b}_{1:n})$ in (4) can be obtained as follows:

[C4] **Batch Quantized (BQ) KF correction step.** Define

$\sigma_y^2(n) := \mathbf{h}^T(n)\mathbf{M}(n \mid \mathbf{b}_{1:n-1})\mathbf{h}(n) + c_v(n)$ and normalized thresholds $\Delta_i(n) := \tau_i(n)/\sigma_y(n)$. Furthermore, define in terms of the conditional mean and variance of the innovation $\tilde{y}(n \mid \mathbf{b}_{1:n-1})$ given $b(n) = i$ the ratios

$$\begin{aligned} \alpha_i(n) &:= \frac{E\{\tilde{y}(n \mid \mathbf{b}_{1:n-1}) \mid \mathbf{b}_{1:n-1}, b(n) = i\}}{\sigma_y(n)} \\ &= \frac{1}{\sqrt{2\pi}} \frac{\exp[-\Delta_i^2(n)/2] - \exp[-\Delta_{i+1}^2(n)/2]}{Q[\Delta_i(n)] - Q[\Delta_{i+1}(n)]} \quad (18) \end{aligned}$$

$$\begin{aligned} \beta_i(n) &:= 1 - \frac{\text{var}\{\tilde{y}(n \mid \mathbf{b}_{1:n-1}) \mid \mathbf{b}_{1:n-1}, b(n) = i\}}{\sigma_y^2(n)} \\ &= \alpha_i^2(n) - \frac{1}{\sqrt{2\pi}} \\ & \quad \times \frac{\Delta_i(n)e^{-\Delta_i^2(n)/2} - \Delta_{i+1}(n)e^{-\Delta_{i+1}^2(n)/2}}{Q[\Delta_i(n)] - Q[\Delta_{i+1}(n)]}. \quad (19) \end{aligned}$$

Then the resultant estimate and its ECM are given by

$$\begin{aligned} \hat{\mathbf{x}}(n \mid \mathbf{b}_{1:n}) &= \hat{\mathbf{x}}(n \mid \mathbf{b}_{1:n-1}) \\ & \quad + \alpha_i(n) \frac{\mathbf{M}(n \mid \mathbf{b}_{1:n-1})\mathbf{h}(n)}{\sqrt{\mathbf{h}^T(n)\mathbf{M}(n \mid \mathbf{b}_{1:n-1})\mathbf{h}(n) + c_v(n)}} \quad (20) \end{aligned}$$

$$\mathbf{M}(n \mid \mathbf{b}_{1:n}) = \mathbf{M}(n \mid \mathbf{b}_{1:n-1})$$

$$- \beta_i(n) \frac{\mathbf{M}(n \mid \mathbf{b}_{1:n-1})\mathbf{h}(n)\mathbf{h}^T(n)\mathbf{M}(n \mid \mathbf{b}_{1:n-1})}{\mathbf{h}^T(n)\mathbf{M}(n \mid \mathbf{b}_{1:n-1})\mathbf{h}(n) + c_v(n)}. \quad (21)$$

Proof: See Appendix A.

Proposition 1 suggests an algorithm for finding (approximate) MMSE state estimates using quantized observations. The resulting batch-quantized Kalman filter (BQKF) consists of recursive application of the prediction step [P3] and the correction step [C4] in a collaborating setting as follows. The active sensor at time n , i.e., the one scheduled to sense $y(n)$ and broadcast a quantized version $b(n)$, is assumed to broadcast within reach of all collaborating sensors. Each sensor, as stated earlier, keeps track of $\mathbf{A}(n)$, $\mathbf{C}_u(n)$, $\mathbf{h}(n)$ and $c_v(n)$ and thus can run the predictor step [P3]. Upon receiving $b(n)$ from the active sensor, all sensors execute the update step [C4].

The BQKF retains a notable resemblance to the clairvoyant KF [P2]–[C2] which is based on analog-amplitude observations. In order to highlight the similarities and differences of the respective correction steps [C2] and [C4], we define $\tilde{\alpha}_i(n \mid \mathbf{b}_{1:n-1}) := \sqrt{\mathbf{h}^T(n)\mathbf{M}(n \mid \mathbf{b}_{1:n-1})\mathbf{h}(n) + c_v(n)}\alpha_i(n)$, $\tilde{\beta}(n) := E\{\beta_i(n) \mid \mathbf{b}_{1:n-1}\}$, and $\tilde{\mathbf{M}}(n \mid \mathbf{b}_{1:n}) := E\{\mathbf{M}(n \mid \mathbf{b}_{1:n}) \mid \mathbf{b}_{1:n-1}\}$. From (20) and (21), it follows that

$$\begin{aligned} \hat{\mathbf{x}}(n \mid \mathbf{b}_{1:n}) &= \hat{\mathbf{x}}(n \mid \mathbf{b}_{1:n-1}) \\ & \quad + \frac{\mathbf{M}(n \mid \mathbf{b}_{1:n-1})\mathbf{h}(n)}{\mathbf{h}^T(n)\mathbf{M}(n \mid \mathbf{b}_{1:n-1})\mathbf{h}(n) + c_v(n)} \tilde{\alpha}_i(n \mid \mathbf{b}_{1:n-1}) \end{aligned}$$

$$\begin{aligned} \tilde{\mathbf{M}}(n \mid \mathbf{b}_{1:n}) &= \mathbf{M}(n \mid \mathbf{b}_{1:n-1}) \\ & \quad - \tilde{\beta}(n) \frac{\mathbf{M}(n \mid \mathbf{b}_{1:n-1})\mathbf{h}(n)\mathbf{h}^T(n)\mathbf{M}(n \mid \mathbf{b}_{1:n-1})}{\mathbf{h}^T(n)\mathbf{M}(n \mid \mathbf{b}_{1:n-1})\mathbf{h}(n) + c_v(n)} \end{aligned}$$

where $\tilde{\alpha}_i(n \mid \mathbf{b}_{1:n-1})$ is the BQKF counterpart of the innovation $\tilde{y}(n \mid \mathbf{y}_{1:n-1})$ in KF [cf. C2] and $\tilde{\beta}(n)$ is obtained from (19) as follows:

$$\begin{aligned} \tilde{\beta}(n) &:= E_{b(n)}\{\beta_i(n) \mid \mathbf{b}_{1:n-1}\} \\ &= \sum_{i=1}^N [Q[\Delta_i(n)] - Q[\Delta_{i+1}(n)]]\beta_i(n) \\ &= \sum_{i=1}^N [Q[\Delta_i(n)] - Q[\Delta_{i+1}(n)]]\alpha_i^2(n). \quad (22) \end{aligned}$$

Remark 1: Comparison of the ECM corrections for the KF in (10) with those for the BQKF in (21) reveal that they are identical except for the $\beta_i(n)$ factor in (21). The similarity is quantified by defining the ECM reduction per correction step [cf. (21)]

$$\begin{aligned} \Delta\mathbf{M}(n) &:= \mathbf{M}(n \mid \mathbf{b}_{1:n-1}) - \mathbf{M}(n \mid \mathbf{b}_{1:n}) \\ &= \beta_i(n) \frac{\mathbf{M}(n \mid \mathbf{b}_{1:n-1})\mathbf{h}(n)\mathbf{h}^T(n)\mathbf{M}(n \mid \mathbf{b}_{1:n-1})}{\mathbf{h}^T(n)\mathbf{M}(n \mid \mathbf{b}_{1:n-1})\mathbf{h}(n) + c_v(n)}. \quad (23) \end{aligned}$$

If we use $y(n)$ instead of $b(n)$ in the correction step, the ECM reduction will be [cf. (10)]

$$\begin{aligned} \Delta\mathbf{M}^K(n) &:= \mathbf{M}(n \mid \mathbf{b}_{1:n-1}) - \mathbf{M}(n \mid \mathbf{b}_{1:n-1}, y(n)) \\ &= \frac{\mathbf{M}(n \mid \mathbf{b}_{1:n-1})\mathbf{h}(n)\mathbf{h}^T(n)\mathbf{M}(n \mid \mathbf{b}_{1:n-1})}{\mathbf{h}^T(n)\mathbf{M}(n \mid \mathbf{b}_{1:n-1})\mathbf{h}(n) + c_v(n)}. \quad (24) \end{aligned}$$

Comparing (23) with (24) we see that $\Delta\mathbf{M}(n) = \beta_i(n)\Delta\mathbf{M}^K(n)$; i.e., the ECM reduction achieved by the BQKF is $\beta_i(n)$ times that of the clairvoyant KF. From (19), $0 < \beta_i(n) < 1$ for any possible selection of thresholds, consistent with the fact that $b(n)$ is a coarse representation of $y(n)$.

A. Quantizer Design for Batch Quantized KF

The ECM $\mathbf{M}(n | \mathbf{b}_{1:n})$ in (21), and consequently the variance reduction $\Delta \mathbf{M}(n)$ in (23), depend on $b(n)$. We define the optimal quantizer as the one that maximizes the average variance reduction, i.e.,

$$\begin{aligned} \{\Delta_i^*(n)\}_{i=2}^N &:= \arg \max_{\{\Delta_i(n)\}_{i=2}^N} E_{b(n)} \{\Delta \mathbf{M}(n) | \mathbf{b}_{1:n-1}\} \\ &= \arg \max_{\{\Delta_i(n)\}_{i=2}^N} E_{b(n)} \{\beta_i(n) | \mathbf{b}_{1:n-1}\} \end{aligned} \quad (25)$$

where $E_{b(n)}\{\cdot | \mathbf{b}_{1:n-1}\}$ denotes expectation with respect to $\Pr\{b(n) | \mathbf{b}_{1:n-1}\}$; and in establishing the second equality we used the fact that given $\mathbf{b}_{1:n-1}$, $\mathbf{M}(n | \mathbf{b}_{1:n-1})$ is conditionally independent of $b(n)$ [cf. (12)]. The last expectation in (25) can be evaluated by substituting $\alpha_i(n)$ from (18) in (22) leading to $\beta(n) := E_{b(n)}\{\beta_i(n) | \mathbf{b}_{1:n-1}\}$

$$= \frac{1}{2\pi} \sum_{i=1}^N \frac{[\exp(-\Delta_i^2(n)/2) - \exp(-\Delta_{i+1}^2(n)/2)]^2}{Q[\Delta_i(n)] - Q[\Delta_{i+1}(n)]}. \quad (26)$$

The optimal thresholds $\{\Delta_i^*(n)\}_{i=2}^N$ in (25) can be obtained as the maximizers of $\beta(n)$ as detailed next in Proposition 2. An alternative approach to the optimal quantization is obtained by using the definition (19), $\sigma_y^2(n)[1 - \beta_i(n)] = \text{var}\{\tilde{y}(n | \mathbf{b}_{1:n-1}) | \mathbf{b}_{1:n-1}, b(n) = i\}$. Proposition 2 shows that the thresholds $\{\Delta_i^*(n)\}_{i=2}^N$ in (25) define the optimal quantizer of the innovation $\tilde{y}(n | \mathbf{b}_{1:n-1})$ with an MSE distortion.

Proposition 2: Consider the problem of optimal quantization of the innovation $\tilde{y}(n | \mathbf{b}_{1:n-1})$. If $b(n) = i$, the reconstructed innovation is $\hat{y}^{(i)}(n | \mathbf{b}_{1:n-1}) := E\{\tilde{y}(n | \mathbf{b}_{1:n-1}) | \mathbf{b}_{1:n-1}, b(n) = i\} = \sigma_y(n) \alpha_i(n)$ [cf. (18)]. We adopt an MSE distortion conditioned on $\mathbf{b}_{1:n-1}$ and define the optimal quantizer of $\tilde{y}(n | \mathbf{b}_{1:n-1})$ as $\{\Delta_i^\dagger(n)\}_{i=2}^N$

$$\begin{aligned} &:= \arg \min_{\{\Delta_i(n)\}_{i=2}^N} d[\tilde{y}(n | \mathbf{b}_{1:n-1}), \hat{y}^{(i)}(n | \mathbf{b}_{1:n-1})] \\ &:= \arg \min_{\{\Delta_i(n)\}_{i=2}^N} E \left\{ \left[\tilde{y}(n | \mathbf{b}_{1:n-1}) - \hat{y}^{(i)}(n | \mathbf{b}_{1:n-1}) \right]^2 | \mathbf{b}_{1:n-1} \right\}. \end{aligned} \quad (27)$$

The optimal thresholds in (25) and (27) are equal, i.e., $\{\Delta_i^*(n)\}_{i=2}^N = \{\Delta_i^\dagger(n)\}_{i=2}^N$.

Proof: Since from definition (19) $\text{var}\{\tilde{y}(n | \mathbf{b}_{1:n-1}) | \mathbf{b}_{1:n-1}, b(n) = i\} = \sigma_y^2(n)[1 - \beta_i(n)]$, $E_{b(n)}\{\text{var}\{\tilde{y}(n | \mathbf{b}_{1:n-1}) | \mathbf{b}_{1:n-1}, b(n)\} | \mathbf{b}_{1:n-1}\} = \sigma_y^2(n)[1 - E_{b(n)}\{\beta_i(n) | \mathbf{b}_{1:n-1}\}]$

it follows that the thresholds that maximize $\beta(n)$ can be obtained from the thresholds that minimize the expectation of the conditional variance, i.e.,

$$\begin{aligned} &\arg \max_{\{\Delta_i(n)\}_{i=2}^N} E_{b(n)}\{\beta_i(n) | \mathbf{b}_{1:n-1}\} \\ &= \arg \min_{\{\Delta_i(n)\}_{i=2}^N} E_{b(n)}\{\text{var}\{\tilde{y}(n | \mathbf{b}_{1:n-1}) | \mathbf{b}_{1:n-1}, b(n) = i\} | \mathbf{b}_{1:n-1}\}. \end{aligned} \quad (28)$$

It remains only to show that the minimization in the second expression of (28) is the conditional MSE of $\hat{y}^{(i)}(n | \mathbf{b}_{1:n-1})$. Writing the variance explicitly with $\mathcal{R}_i := [\tau_i(n), \tau_{i+1}(n))$, we have $\text{var}\{\tilde{y}(n | \mathbf{b}_{1:n-1}) | \mathbf{b}_{1:n-1}, b(n) = i\}$

$$\begin{aligned} &= \int_{\mathcal{R}_i} [\tilde{y}(n | \mathbf{b}_{1:n-1}) - E\{\tilde{y}(n | \mathbf{b}_{1:n-1}) | \mathbf{b}_{1:n-1}, b(n) = i\}]^2 \\ &\quad \times p[\tilde{y}(n | \mathbf{b}_{1:n-1}) | \mathbf{b}_{1:n-1}, b(n) = i] d\tilde{y}(n | \mathbf{b}_{1:n-1}). \end{aligned} \quad (29)$$

Given that $E\{\tilde{y}(n | \mathbf{b}_{1:n-1}) | \mathbf{b}_{1:n-1}, b(n) = i\} = \hat{y}^{(i)}(n | \mathbf{b}_{1:n-1})$ the conditional expectation of (29) is written as

$$\begin{aligned} &E_{b(n)}\{\text{var}\{\tilde{y}(n | \mathbf{b}_{1:n-1}) | \mathbf{b}_{1:n-1}, b(n) = i\} | \mathbf{b}_{1:n-1}\} \\ &= \sum_{i=1}^N \int_{\mathcal{R}_i} [\tilde{y}(n | \mathbf{b}_{1:n-1}) - \hat{y}^{(i)}(n | \mathbf{b}_{1:n-1})]^2 \\ &\quad \times p[\tilde{y}(n | \mathbf{b}_{1:n-1}) | \mathbf{b}_{1:n-1}, b(n) = i] d\tilde{y}(n | \mathbf{b}_{1:n-1}) \\ &\quad \times \Pr\{b(n) = i | \mathbf{b}_{1:n-1}\}. \end{aligned} \quad (30)$$

Since $p[\tilde{y}(n | \mathbf{b}_{1:n-1}) | \mathbf{b}_{1:n-1}, b(n) = i] = 0$ for $\tilde{y}(n | \mathbf{b}_{1:n-1}) \notin \mathcal{R}_i$, then $p[\tilde{y}(n | \mathbf{b}_{1:n-1}) | \mathbf{b}_{1:n-1}, b(n) = i] \Pr\{b(n) = i | \mathbf{b}_{1:n-1}\} = p[\tilde{y}(n | \mathbf{b}_{1:n-1}) | \mathbf{b}_{1:n-1}]$ if $\tilde{y}(n | \mathbf{b}_{1:n-1}) \in \mathcal{R}_i$, and zero otherwise. Thus, (30) can be written as

$$\begin{aligned} &E_{b(n)}\{\text{var}\{\tilde{y}(n | \mathbf{b}_{1:n-1}) | \mathbf{b}_{1:n-1}, b(n) = i\} | \mathbf{b}_{1:n-1}\} \\ &= \sum_{i=1}^N \int_{\mathcal{R}_i} [\tilde{y}(n | \mathbf{b}_{1:n-1}) - \hat{y}^{(i)}(n | \mathbf{b}_{1:n-1})]^2 \\ &\quad \times p[\tilde{y}(n | \mathbf{b}_{1:n-1}) | \mathbf{b}_{1:n-1}] d\tilde{y}(n | \mathbf{b}_{1:n-1}) \\ &= d[\tilde{y}(n | \mathbf{b}_{1:n-1}), \hat{y}^{(i)}(n | \mathbf{b}_{1:n-1})] \end{aligned}$$

where the second equality comes from the definition of the distortion metric in (27). Since the optimization arguments in (25) and (27) are equal the proof follows. ■

We emphasize the subtle difference between the thresholds $\{\Delta_i^*(n)\}_{i=2}^N$ in (25) and $\{\Delta_i^\dagger(n)\}_{i=2}^N$ in (27). While the former minimizes the MSE of the state estimates $\hat{\mathbf{x}}(n | \mathbf{b}_{1:n})$, the latter minimizes the reconstruction error when estimating the innovation $\tilde{y}(n | \mathbf{b}_{1:n-1})$ by $\hat{y}^{(i)}(n | \mathbf{b}_{1:n-1})$. Even though these two criteria are different, the corresponding optimal thresholds coincide. Indeed, Proposition 2 asserts that the optimal strategy for estimating $\hat{\mathbf{x}}(n | \mathbf{b}_{1:n})$ is to quantize $\tilde{y}(n | \mathbf{b}_{1:n-1})$ with minimum MSE distortion.

The optimization problem in (27) has a well known solution given by the Lloyd-Max quantizer [14], [16]. Since $p[\tilde{y}(n | \mathbf{b}_{1:n-1}) | \mathbf{b}_{1:n-1}] \approx \mathcal{N}[\tilde{y}(n | \mathbf{b}_{1:n-1}); 0, \sigma_y^2(n)]$, the use of normalized thresholds $\Delta_i := \tau_i(n)/\sigma_y(n)$ leads to quantization of $\tilde{y}(n | \mathbf{b}_{1:n-1})/\sigma_y(n)$ which corresponds to quantization of zero-mean, unit variance Gaussian random variables. The optimal normalized thresholds values for $N = 2$, $N = 4$, $N = 8$, and $N = 16$, from [16], are given in Table I and the corresponding $\bar{\beta}(n)$ obtained using (26) are summarized in Table II. We can see that even quantizing to a single bit has $\bar{\beta}(n) = 2/\pi \approx 0.64$ and quantizing to more than 4 bits, for which $\bar{\beta}(n) \approx 0.99$, seems rather unjustified.

B. Binary Quantized Kalman Filter (1-QKF)

A particularly interesting case results when $N = 2$, which amounts to binary quantization. In this case, there is a single threshold $\tau(n) := \tau_2(n)$ to be determined (since $\tau_1(n) = -\infty$ and $\tau_3(n) = +\infty$), and we have $\mathcal{R}_1 = (-\infty, \tau(n))$ and $\mathcal{R}_2 = [\tau(n), +\infty)$. Upon defining $\Delta(n) := \tau(n)/[\mathbf{h}^T(n)\mathbf{M}(n | \mathbf{b}_{1:n-1})\mathbf{h}(n) + c_v(n)]^{1/2}$ the variables $\alpha_{1,2}(n)$ and $\beta_{1,2}(n)$ take on simpler expressions given by [cf. (18) and (19)]

$$\alpha_{1,2}(n) = \mp \frac{1}{\sqrt{2\pi}} \frac{\exp[-\Delta^2(n)/2]}{Q[\mp\Delta(n)]}$$

TABLE I
QUANTIZATION THRESHOLDS FOR GAUSSIAN PDF, $\Delta_i = -\Delta_{N+2-i}, \forall i \in \{1, 2, \dots, N\}$

N	Δ_2	Δ_3	N	Δ_3	Δ_4	Δ_5	N	Δ_5	Δ_6	Δ_7	Δ_8	Δ_9
2	0	∞	4	0	0.982	∞	8	0	0.501	1.050	1.748	∞
N	Δ_9	Δ_{10}	Δ_{11}	Δ_{12}	Δ_{13}	Δ_{14}	Δ_{15}	Δ_{16}	Δ_{17}			
16	0	0.258	0.522	0.800	1.099	1.437	1.844	2.401	∞			

TABLE II
 $\bar{\beta}(n)$ VALUES FOR BATCH QUANTIZATION

N ($\log_2(N)$)	2 (1 bit)	4 (2 bits)	8 (3 bits)	16 (4 bits)
$\bar{\beta}(n)$	0.637=2/ π	0.883	0.966	0.991

$$\beta_{1,2}(n) = \alpha_{1,2}^2(n) \pm \frac{1}{\sqrt{2\pi}} \frac{\Delta(n) \exp[-\Delta^2(n)/2]}{Q[\mp\Delta(n)]}$$

where \mp signifies the use of minus for $b(n) = 1$ and plus for $b(n) = 2$ (and *vice versa* for \pm). Interestingly, the expected performance factor simplifies to [cf. (26)]

$$\bar{\beta}(n) = \frac{1}{2\pi} \left[\frac{\exp^2[-\Delta^2(n)/2]}{Q[\Delta(n)]} + \frac{\exp^2[-\Delta^2(n)/2]}{Q[-\Delta(n)]} \right] \\ = \frac{1}{2\pi} \frac{\exp[-\Delta^2(n)]}{Q[\Delta(n)]Q[-\Delta(n)]}. \quad (31)$$

Appendix C shows that $\Delta(n) = 0$ maximizes $\bar{\beta}(n)$ in (31). With $\Delta(n) = 0$, $\bar{\beta}(n) = 2/\pi$, corroborating the result for $N = 2$ in Table II. For the optimally selected threshold $\tau(n) = 0$ it is convenient to change the notation and define the message, $b(n)$ in (14), as the sign of the innovation

$$b(n) = \text{sign}[\tilde{y}(n | \mathbf{b}_{1:n-1})] \quad (32)$$

which is equivalent to $b(n) = -1$ if $\tilde{y}(n | \mathbf{b}_{1:n-1}) \in \mathcal{R}_1$ and $b(n) = +1$ if $\tilde{y}(n | \mathbf{b}_{1:n-1}) \in \mathcal{R}_2$. In this case, the correction step [C4] takes on the rather simple form presented next.

[C5] **1-bit quantized KF (1-QKF) correction step.** The state estimate and ECM are given by

$$\hat{\mathbf{x}}(n | \mathbf{b}_{1:n}) = \hat{\mathbf{x}}(n | \mathbf{b}_{1:n-1}) \\ + \sqrt{\frac{2}{\pi}} \frac{\mathbf{M}(n | \mathbf{b}_{1:n-1})\mathbf{h}(n)}{\sqrt{\mathbf{h}^T(n)\mathbf{M}(n | \mathbf{b}_{1:n-1})\mathbf{h}(n) + c_v(n)}} b(n) \quad (33)$$

$$\mathbf{M}(n | \mathbf{b}_{1:n}) = \mathbf{M}(n | \mathbf{b}_{1:n-1}) \\ - \frac{2}{\pi} \frac{\mathbf{M}(n | \mathbf{b}_{1:n-1})\mathbf{h}(n)\mathbf{h}^T(n)\mathbf{M}(n | \mathbf{b}_{1:n-1})}{\mathbf{h}^T(n)\mathbf{M}(n | \mathbf{b}_{1:n-1})\mathbf{h}(n) + c_v(n)}. \quad (34)$$

The iteration [P3]-[C5] is the Sign of Innovations KF (SoI-KF) introduced in [21]. The simplicity of [C5] suggests an alternative approach for iterative multi-bit quantization which is pursued in the next section.

IV. ITERATIVELY QUANTIZED KALMAN FILTER

In this section's iteratively quantized Kalman filter (IQKF), sensors rely on m -bit binary messages $\mathbf{b}(n) := \mathbf{b}^{(1:m)}(n) := [b^{(1)}(n), \dots, b^{(m)}(n)]$, with the i th bit $b^{(i)}(n)$ defined as the sign of innovations [cf. (36)] conditioned on the previous messages $\mathbf{b}_{1:n-1} := [\mathbf{b}(1), \dots, \mathbf{b}(n-1)]$ and previous bits $\mathbf{b}^{(1:i-1)}(n) := [b^{(1)}(n), \dots, b^{(i-1)}(n)]$ of the current (n)th message. Specifically, let

$$\hat{y}^{(0)}(n | \mathbf{b}_{1:n-1}) := \hat{y}(n | \mathbf{b}_{1:n-1}) = \mathbb{E}\{y(n) | \mathbf{b}_{1:n-1}\} \\ \hat{y}^{(i)}(n | \mathbf{b}_{1:n-1}) := \mathbb{E}\left\{y(n) | \mathbf{b}_{1:n-1}, \mathbf{b}^{(1:i)}(n)\right\}, \\ \text{for } i \geq 1 \quad (35)$$

stand for MMSE estimates of $y(n)$ using past messages $\mathbf{b}_{1:n-1}$ and the first i bits of the current message denoted as $\mathbf{b}^{(1:i)}(n)$. The i th bit of the current message, $b^{(i)}(n)$, is obtained as

$$b^{(i)}(n) := \text{sign}\left[y(n) - \hat{y}^{(i-1)}(n | \mathbf{b}_{1:n-1})\right] \\ := \text{sign}\left[\tilde{y}^{(i-1)}(n | \mathbf{b}_{1:n-1})\right]. \quad (36)$$

Our goal here is to derive an iterative algorithm to obtain estimates

$$\hat{\mathbf{x}}^{(i)}(n | \mathbf{b}_{1:n-1}) := \mathbb{E}\left\{\mathbf{x}(n) | \mathbf{b}_{1:n-1}, \mathbf{b}^{(1:i)}(n)\right\} \quad (37)$$

based on $\hat{\mathbf{x}}^{(i-1)}(n | \mathbf{b}_{1:n-1})$ and $b^{(i)}(n)$. When using m bits, $\mathbf{b}^{(1:m)}(n)$, we will refer to the resulting algorithm as m-IQKF.

At this point we should note that the 1-IQKF coincides with the BQKF with $N = 2$ quantization regions and optimally selected threshold $\tau(n) = 0$, as in Section III-B. Thus, when $m = 1$ the estimates in (37) can be obtained using the iteration [P2]-[C5]. Since the definition of $b^{(i)}(n)$ is a straightforward extension of the corresponding definition for the 1-QKF [cf. (36) and (32)], one option for $i \geq 1$ would be to set $\hat{y}^{(i)}(n | \mathbf{b}_{1:n-1})$ equal to $\mathbf{h}^T(n)\hat{\mathbf{x}}^{(i)}(n | \mathbf{b}_{1:n-1})$ and then apply iterative correction steps of the form [C5]. However, $\hat{y}^{(i)}(n | \mathbf{b}_{1:n-1}) \neq \mathbf{h}^T(n)\hat{\mathbf{x}}^{(i)}(n | \mathbf{b}_{1:n-1})$ if $i \geq 1$ as explained next. Using the observations (2), the definitions of $\hat{y}^{(i)}(n | \mathbf{b}_{1:n-1})$ in (35) and $\hat{\mathbf{x}}^{(i)}(n | \mathbf{b}_{1:n-1})$ in (37), we obtain

$$\hat{y}^{(i)}(n | \mathbf{b}_{1:n-1}) = \mathbb{E}\left\{\mathbf{h}^T(n)\mathbf{x}(n) + v(n) | \mathbf{b}_{1:n-1}, \mathbf{b}^{(1:i)}(n)\right\} \\ = \mathbf{h}^T(n)\hat{\mathbf{x}}^{(i)}(n | \mathbf{b}_{1:n-1}) + \mathbb{E}\left\{v(n) | \mathbf{b}_{1:n-1}, \mathbf{b}^{(1:i)}(n)\right\}. \quad (38)$$

The noise estimate $\mathbb{E}\{v(n) | \mathbf{b}_{1:n-1}, \mathbf{b}^{(1:i)}(n)\}$ is not necessarily zero for $i \geq 1$; see also (48). (The converse is true for the 1-IQKF where $\mathbb{E}\{v(n) | \mathbf{b}_{1:n-1}\} = \mathbb{E}\{v(n)\} = 0$.) Therefore, in order to obtain $\hat{y}^{(i)}(n | \mathbf{b}_{1:n-1})$ we need $\hat{\mathbf{x}}^{(i)}(n | \mathbf{b}_{1:n-1})$ as well as $\mathbb{E}\{v(n) | \mathbf{b}_{1:n-1}, \mathbf{b}^{(1:i)}(n)\}$. In order to keep track of the noise estimate and its covariance, we augment the state with the noise as described in the next section.

A. State Augmentation

Through state augmentation the estimates $\mathbb{E}\{v(n) | \mathbf{b}_{1:n-1}, \mathbf{b}^{(1:i)}(n)\}$ can be obtained so that the predicted observation $\hat{y}^{(i)}(n | \mathbf{b}_{1:n-1})$ in (38) can be evaluated even for $i > 1$ (i.e., multi-bit quantization). Specifically, appending observation noise $v(n)$ to the state vector $\mathbf{x}(n)$ we construct an augmented state vector $\check{\mathbf{x}}(n) := [\mathbf{x}^T(n), v(n)]^T$. Correspondingly, we define augmented driving noise $\check{\mathbf{u}}(n) := [\mathbf{u}^T(n), v(n)]^T$, state

propagation matrix $\check{\mathbf{A}}(n) := \begin{pmatrix} \mathbf{A}(n) & \mathbf{0} \\ \mathbf{0}^T & 0 \end{pmatrix}$ and observation vector $\check{\mathbf{h}}(n) := [\mathbf{h}^T(n), 1]^T$. The model in (1)-(2) can, consequently, be rewritten with the following augmented state and observation equations

$$\check{\mathbf{x}}(n) = \check{\mathbf{A}}(n)\check{\mathbf{x}}(n-1) + \check{\mathbf{u}}(n) \quad (39)$$

$$\check{y}(n) = \check{\mathbf{h}}^T(n)\check{\mathbf{x}}(n) + \check{v}(n) \quad (40)$$

where the new observation noise $\check{v}(n) = 0, \forall n$ (by construction) and can be thought of as Gaussian noise with variance $c_v(n) = 0$. Note that the covariance matrix of the augmented driving noise is a block-diagonal matrix $\mathbf{C}_{\check{\mathbf{u}}}(n) \in \mathbb{R}^{(p+1) \times (p+1)}$ with $[\mathbf{C}_{\check{\mathbf{u}}}(n)]_{1:p,1:p} = \mathbf{C}_{\mathbf{u}}(n)$ and $[\mathbf{C}_{\check{\mathbf{u}}}(n)]_{p+1,p+1} = c_v(n)$.

The augmented state formulation (39)–(40) increases the dimension of the state vector but is otherwise equivalent to (1)–(2). However, it has the appealing property that MMSE estimates of the augmented state $\check{\mathbf{x}}(n)$ contain MMSE estimates of the original state $\mathbf{x}(n)$ and the observation noise $v(n)$. In particular, state-augmentation allows simple computation of $\hat{y}^{(i)}(n | \mathbf{b}_{1:n-1})$ in (35) as detailed in the following lemma:

Lemma 1: Consider the augmented state MMSE estimate $\hat{\mathbf{x}}^{(i)}(n | \mathbf{b}_{1:n-1}) = \mathbb{E}\{\check{\mathbf{x}}(n) | \mathbf{b}_{1:n-1}, \mathbf{b}^{(1:i)}(n)\}$ and the predicted augmented observation estimate $\hat{y}^{(i)}(n | \mathbf{b}_{1:n-1}) = \mathbb{E}\{\check{y}(n) | \mathbf{b}_{1:n-1}, \mathbf{b}^{(1:i)}(n)\}$. The predicted observation MMSE estimate $\hat{y}^{(i)}(n | \mathbf{b}_{1:n-1})$ in (35) can be obtained as

$$\hat{y}^{(i)}(n | \mathbf{b}_{1:n-1}) = \hat{y}^{(i)}(n | \mathbf{b}_{1:n-1}) = \check{\mathbf{h}}^T(n)\hat{\mathbf{x}}^{(i)}(n | \mathbf{b}_{1:n-1}). \quad (41)$$

Proof: The observation $y(n)$ in (2) and the augmented observation $\check{y}(n)$ in (40) are the same by construction. That is,

$$\begin{aligned} \check{y}(n) &= \check{\mathbf{h}}^T(n)\check{\mathbf{x}}(n) + \check{v}(n) = \check{\mathbf{h}}^T(n)\check{\mathbf{x}}(n) \\ &= \mathbf{h}^T(n)\mathbf{x}(n) + v(n) = y(n) \end{aligned} \quad (42)$$

where the first equality follows from (40), the second one from $\check{v}(n) = 0$, the third one from the definitions of $\check{\mathbf{h}}(n)$ and $\check{\mathbf{x}}(n)$, and the last one from (2). Taking expectation with respect to $p[y(n) | \mathbf{b}_{1:n-1}, \mathbf{b}^{(1:i)}(n)]$ in the first, third and fifth terms of the equality in (42) results in (41). ■

Based on Lemma 1 we can now use the augmented state estimates to find the observation estimates. Combining this with the 1-QKF recursion [P3]–[C5], we obtain the MMSE estimates in (37) using the algorithm detailed in the next proposition.

Proposition 3: Consider the augmented state space model in (39) and (40). Define the augmented state estimates $\hat{\mathbf{x}}(n | \mathbf{b}_{1:n-1}) := \mathbb{E}\{\check{\mathbf{x}}(n) | \mathbf{b}_{1:n-1}\}$ and for $i = 1, \dots, m$, $\hat{\mathbf{x}}^{(i-1)}(n | \mathbf{b}_{1:n-1}) := \mathbb{E}\{\check{\mathbf{x}}(n) | \mathbf{b}_{1:n-1}, \mathbf{b}^{(1:i-1)}(n)\}$. Define the corresponding ECMs as $\check{\mathbf{M}}(n | \mathbf{b}_{1:n-1}) := \mathbb{E}\{[\check{\mathbf{x}}(n | \mathbf{b}_{1:n-1}) - \hat{\mathbf{x}}(n | \mathbf{b}_{1:n-1})][\check{\mathbf{x}}(n | \mathbf{b}_{1:n-1}) - \hat{\mathbf{x}}(n | \mathbf{b}_{1:n-1})]^T\}$ and $\check{\mathbf{M}}^{(i-1)}(n | \mathbf{b}_{1:n-1}) := \mathbb{E}\{[\hat{\mathbf{x}}^{(i-1)}(n | \mathbf{b}_{1:n-1}) - \hat{\mathbf{x}}(n | \mathbf{b}_{1:n-1})][\hat{\mathbf{x}}^{(i-1)}(n | \mathbf{b}_{1:n-1}) - \hat{\mathbf{x}}(n | \mathbf{b}_{1:n-1})]^T\}$. Construct the messages $\mathbf{b}^{(1:m)}(n)$ [cf. (36)] as

$$b^{(i)}(n) := \text{sign} \left[y(n) - \check{\mathbf{h}}^T(n)\hat{\mathbf{x}}^{(i-1)}(n | \mathbf{b}_{1:n-1}) \right]. \quad (43)$$

Furthermore, find the estimate $\hat{\mathbf{x}}^{(i)}(n | \mathbf{b}_{1:n-1})$ from the following recursion:

[P4] Given the previous estimate $\hat{\mathbf{x}}(n-1 | \mathbf{b}_{1:n-1})$ and its ECM $\check{\mathbf{M}}(n-1 | \mathbf{b}_{1:n-1})$, form

$$\hat{\mathbf{x}}(n | \mathbf{b}_{1:n-1}) = \check{\mathbf{A}}(n)\hat{\mathbf{x}}(n-1 | \mathbf{b}_{1:n-1}) \quad (44)$$

$$\check{\mathbf{M}}(n | \mathbf{b}_{1:n-1}) = \check{\mathbf{A}}(n)\check{\mathbf{M}}(n-1 | \mathbf{b}_{1:n-1})\check{\mathbf{A}}^T(n) + \mathbf{C}_{\check{\mathbf{u}}}(n). \quad (45)$$

[C6] Assuming that $p[\check{\mathbf{x}}(n) | \mathbf{b}_{1:n-1}, \mathbf{b}^{(1:i-1)}(n)] = \mathcal{N}[\check{\mathbf{x}}(n); \hat{\mathbf{x}}^{(i-1)}(n | \mathbf{b}_{1:n-1}), \check{\mathbf{M}}^{(i-1)}(n | \mathbf{b}_{1:n-1})]$, the MMSE estimate $\hat{\mathbf{x}}^{(i)}(n | \mathbf{b}_{1:n-1}) := \mathbb{E}\{\check{\mathbf{x}}(n) | \mathbf{b}_{1:n-1}, \mathbf{b}^{(1:i)}(n)\}$ and the corresponding ECM $\check{\mathbf{M}}^{(i)}(n | \mathbf{b}_{1:n-1})$ are obtained by iterative application of

$$\begin{aligned} \hat{\mathbf{x}}^{(i)}(n | \mathbf{b}_{1:n-1}) &= \hat{\mathbf{x}}^{(i-1)}(n | \mathbf{b}_{1:n-1}) \\ &+ \sqrt{\frac{2}{\pi}} \frac{\check{\mathbf{M}}^{(i-1)}(n | \mathbf{b}_{1:n-1})\check{\mathbf{h}}(n)}{\sqrt{\check{\mathbf{h}}^T(n)\check{\mathbf{M}}^{(i-1)}(n | \mathbf{b}_{1:n-1})\check{\mathbf{h}}(n)}} b^{(i)}(n) \end{aligned} \quad (46)$$

$$\begin{aligned} \check{\mathbf{M}}^{(i)}(n | \mathbf{b}_{1:n-1}) &= \check{\mathbf{M}}^{(i-1)}(n | \mathbf{b}_{1:n-1}) \\ &- \frac{2}{\pi} \frac{\check{\mathbf{M}}^{(i-1)}(n | \mathbf{b}_{1:n-1})\check{\mathbf{h}}(n)\check{\mathbf{h}}^T(n)\check{\mathbf{M}}^{(i-1)}(n | \mathbf{b}_{1:n-1})}{\check{\mathbf{h}}^T(n)\check{\mathbf{M}}^{(i-1)}(n | \mathbf{b}_{1:n-1})\check{\mathbf{h}}(n)} \end{aligned} \quad (47)$$

where we used the definitions $\hat{\mathbf{x}}^{(0)}(n | \mathbf{b}_{1:n-1}) := \hat{\mathbf{x}}(n | \mathbf{b}_{1:n-1})$ and $\check{\mathbf{M}}^{(0)}(n | \mathbf{b}_{1:n-1}) := \check{\mathbf{M}}(n | \mathbf{b}_{1:n-1})$. For time index n , (46) and (47) are repeated m -times.

The MMSE estimate of $\check{\mathbf{x}}(n)$ given $\mathbf{b}_{1:n}$ is $\hat{\mathbf{x}}(n | \mathbf{b}_{1:n}) = \mathbb{E}\{\check{\mathbf{x}}(n) | \mathbf{b}_{1:n}\} = \mathbb{E}\{\check{\mathbf{x}}(n) | \mathbf{b}_{1:n-1}, \mathbf{b}^{(1:m)}(n)\} = \hat{\mathbf{x}}^{(m)}(n | \mathbf{b}_{1:n-1})$. The corresponding ECM is $\check{\mathbf{M}}(n | \mathbf{b}_{1:n}) := \check{\mathbf{M}}^{(m)}(n | \mathbf{b}_{1:n-1})$.

Proof: See Appendix B.

The state estimates $\hat{\mathbf{x}}^{(i)}(n | \mathbf{b}_{1:n-1})$ in (37) are the first p components of the augmented state estimate $\hat{\mathbf{x}}^{(i)}(n | \mathbf{b}_{1:n-1})$, i.e., $\hat{\mathbf{x}}^{(i)}(n | \mathbf{b}_{1:n-1}) = [\hat{\mathbf{x}}^{(i)}(n | \mathbf{b}_{1:n-1})]_{1:p}$ and the noise estimate is the $(p+1)$ th component $\mathbb{E}\{v(n) | \mathbf{b}_{1:n-1}, \mathbf{b}^{(1:i)}(n)\} = [\hat{\mathbf{x}}^{(i)}(n | \mathbf{b}_{1:n-1})]_{p+1}$.

Corollary 1: For $i = 1$, $\mathbb{E}\{v(n) | \mathbf{b}_{1:n-1}, \mathbf{b}^{(1:i)}(n)\} \neq 0$.

Proof: The $(p+1)$ th entry of $\hat{\mathbf{x}}^{(i)}(n | \mathbf{b}_{1:n-1})$ in (46) is the noise estimate $\mathbb{E}\{v(n) | \mathbf{b}_{1:n-1}, \mathbf{b}^{(1:i)}(n)\}$. Thus, for $i = 1$ $\mathbb{E}\{v(n) | \mathbf{b}_{1:n-1}, b(n)\}$

$$\begin{aligned} &= \mathbb{E}\{v(n) | \mathbf{b}_{1:n-1}\} + \sqrt{\frac{2}{\pi}} \frac{[\check{\mathbf{M}}^{(0)}(n | \mathbf{b}_{1:n-1})\check{\mathbf{h}}(n)]_{p+1}}{\sqrt{\check{\mathbf{h}}^T(n)\check{\mathbf{M}}^{(0)}(n | \mathbf{b}_{1:n-1})\check{\mathbf{h}}(n)}} b(n) \\ &= \sqrt{\frac{2}{\pi}} \frac{c_v(n)}{\sqrt{\check{\mathbf{h}}^T(n)\check{\mathbf{M}}(n | \mathbf{b}_{1:n-1})\check{\mathbf{h}}(n) + c_v(n)}} b(n) \neq 0. \end{aligned} \quad (48)$$

The last equality follows since $\mathbb{E}\{v(n) | \mathbf{b}_{1:n-1}\} = \mathbb{E}\{v(n)\} = 0$ and $[\check{\mathbf{M}}^{(0)}(n | \mathbf{b}_{1:n-1})\check{\mathbf{h}}(n)]_{p+1} = c_v(n)$. ■

The similarity of the m-IQKF in Proposition 3 with the clairvoyant KF based on un-quantized observations (cf. [P2]–[C2]) is even more remarkable than the similarity between BQKF and KF. As in the BQKF, the ECM updates in (47) are identical to the ECM updates of the KF except for the scale factor $2/\pi$, suggesting that the MSE penalty due to quantization is small. The ECMs of the m-IQKF iterates are independent of the message sequence $\mathbf{b}_{1:m}$, which is not the case for the BQKF. This property shared by the KF strengthens the variance performance claims of the m-IQKF. While the small variance penalty factors summarized in Table II are valid on average for BQKF, the variance penalty factors of the m-IQKF hold true for all message sequences $\mathbf{b}_{1:n}$. The variance penalties associated with m-IQKF are investigated in the following corollaries.

Corollary 2: Consider the m-IQKF algorithm in Proposition 3 and define the ECM reduction after $i = 1, \dots, m$ iterations as $\Delta\check{\mathbf{M}}_i(n) := \check{\mathbf{M}}^{(0)}(n | \mathbf{b}_{1:n-1}) - \check{\mathbf{M}}^{(i)}(n | \mathbf{b}_{1:n-1})$, where $\check{\mathbf{M}}^{(0)}(n | \mathbf{b}_{1:n-1}) := \check{\mathbf{M}}(n | \mathbf{b}_{1:n-1})$. With $c_i := 1 -$

TABLE III
PER STEP FACTOR, c_m , FOR ITERATIVE QUANTIZATION

bits, m	1	2	3	4
c_m	0.637=2/π	0.868	0.952	0.983

$(1 - (2/\pi))^i$, the error covariance reduction after i iterations is given as

$$\Delta\check{\mathbf{M}}_i(n) = c_i \frac{\check{\mathbf{M}}^{(0)}(n | \mathbf{b}_{1:n-1}) \check{\mathbf{h}}(n) \check{\mathbf{h}}^T(n) \check{\mathbf{M}}^{(0)}(n | \mathbf{b}_{1:n-1})}{\check{\mathbf{h}}^T(n) \check{\mathbf{M}}^{(0)}(n | \mathbf{b}_{1:n-1}) \check{\mathbf{h}}(n)}. \quad (49)$$

Proof: We first write $\Delta\check{\mathbf{M}}_i(n)$ as a summation of differences between successive ECM matrices

$$\begin{aligned} \Delta\check{\mathbf{M}}_i(n) &:= \check{\mathbf{M}}^{(0)}(n | \mathbf{b}_{1:n-1}) - \check{\mathbf{M}}^{(i)}(n | \mathbf{b}_{1:n-1}) \\ &= \sum_{j=1}^i [\check{\mathbf{M}}^{(j-1)}(n | \mathbf{b}_{1:n-1}) - \check{\mathbf{M}}^{(j)}(n | \mathbf{b}_{1:n-1})] \\ &= \frac{2}{\pi} \sum_{j=1}^i \left[\frac{\check{\mathbf{M}}^{(j-1)}(n | \mathbf{b}_{1:n-1}) \check{\mathbf{h}}(n) \check{\mathbf{h}}^T(n) \check{\mathbf{M}}^{(j-1)}(n | \mathbf{b}_{1:n-1})}{\check{\mathbf{h}}^T(n) \check{\mathbf{M}}^{(j-1)}(n | \mathbf{b}_{1:n-1}) \check{\mathbf{h}}(n)} \right] \end{aligned} \quad (50)$$

where the last equality follows from (47). Next, we recursively obtain the product $\check{\mathbf{M}}^{(i)}(n | \mathbf{b}_{1:n-1}) \check{\mathbf{h}}(n)$ by multiplying the ECM in (47) by $\check{\mathbf{h}}(n)$ to obtain

$$\check{\mathbf{M}}^{(i)}(n | \mathbf{b}_{1:n-1}) \check{\mathbf{h}}(n) = \check{\mathbf{M}}^{(i-1)}(n | \mathbf{b}_{1:n-1}) \check{\mathbf{h}}(n) - \frac{2 \check{\mathbf{M}}^{(i-1)}(n | \mathbf{b}_{1:n-1}) \check{\mathbf{h}}(n) \check{\mathbf{h}}^T(n) \check{\mathbf{M}}^{(i-1)}(n | \mathbf{b}_{1:n-1}) \check{\mathbf{h}}(n)}{\pi \check{\mathbf{h}}^T(n) \check{\mathbf{M}}^{(i-1)}(n | \mathbf{b}_{1:n-1}) \check{\mathbf{h}}(n)} \quad (51)$$

$$= \left(1 - \frac{2}{\pi}\right) \check{\mathbf{M}}^{(i-1)}(n | \mathbf{b}_{1:n-1}) \check{\mathbf{h}}(n) \quad (52)$$

where we cancelled out factors $\check{\mathbf{h}}^T(n) \check{\mathbf{M}}^{(i)}(n | \mathbf{b}_{1:n-1}) \check{\mathbf{h}}(n)$ in the numerator and denominator of the second term in (51). Repeating steps (51)–(52) for $\check{\mathbf{M}}^{(i-1)}(n | \mathbf{b}_{1:n-1}) \check{\mathbf{h}}(n)$ with decreasing index i yields

$$\check{\mathbf{M}}^{(i)}(n | \mathbf{b}_{1:n-1}) \check{\mathbf{h}}(n) = \left(1 - \frac{2}{\pi}\right)^i \check{\mathbf{M}}^{(0)}(n | \mathbf{b}_{1:n-1}) \check{\mathbf{h}}(n).$$

Thus, substituting $\check{\mathbf{M}}^{(j-1)}(n | \mathbf{b}_{1:n-1}) \check{\mathbf{h}}(n) = (1 - (2/\pi))^{j-1} \check{\mathbf{M}}^{(0)}(n | \mathbf{b}_{1:n-1}) \check{\mathbf{h}}(n)$ into (50) yields

$$\begin{aligned} \Delta\check{\mathbf{M}}_i(n) &= \frac{2}{\pi} \left[\sum_{j=1}^i \left(1 - \frac{2}{\pi}\right)^{j-1} \right] \\ &\quad \times \frac{\check{\mathbf{M}}^{(0)}(n | \mathbf{b}_{1:n-1}) \check{\mathbf{h}}(n) \check{\mathbf{h}}^T(n) \check{\mathbf{M}}^{(0)}(n | \mathbf{b}_{1:n-1})}{\check{\mathbf{h}}^T(n) \check{\mathbf{M}}^{(0)}(n | \mathbf{b}_{1:n-1}) \check{\mathbf{h}}(n)} \end{aligned}$$

and upon invoking the geometric sum identity

$$(2/\pi) \sum_{j=1}^i (1 - (2/\pi))^{j-1} = 1 - (1 - (2/\pi))^i,$$

(49) follows. \blacksquare

For the clairvoyant KF based on un-quantized observations the ECM reduction $\Delta\check{\mathbf{M}}^K(n)$ is given by (24), and can be seen to correspond to the reduction $\Delta\check{\mathbf{M}}_i(n)$ in (49) with $c_m = 1$. Therefore, Corollary 2 asserts that the ECM reduction achieved by quantizing to m bits is c_m times smaller than the

one achieved with analog-amplitude observations. Values of c_m are shown in Table III. With only 4 quantization bits, the value of c_m is just 2% less than the value for the clairvoyant KF ($c_m = 1$).

Using Corollary 2 we can relate the predicted MSE $\text{tr}\{\check{\mathbf{M}}(n | \mathbf{b}_{1:n-1})\}$ and the corrected MSE $\text{tr}\{\check{\mathbf{M}}(n | \mathbf{b}_{1:n})\}$ after using the m bits of the n th observation, $\mathbf{b}^{(1:m)}(n)$. Corollary 3 summarizes this result.

Corollary 3: *The predicted and corrected ECMs of the m-IQKF are related as*

$$\check{\mathbf{M}}(n | \mathbf{b}_{1:n}) = \check{\mathbf{M}}(n | \mathbf{b}_{1:n-1}) - c_m \frac{\check{\mathbf{M}}(n | \mathbf{b}_{1:n-1}) \check{\mathbf{h}}(n) \check{\mathbf{h}}^T(n) \check{\mathbf{M}}(n | \mathbf{b}_{1:n-1})}{\check{\mathbf{h}}^T(n) \check{\mathbf{M}}(n | \mathbf{b}_{1:n-1}) \check{\mathbf{h}}(n)} \quad (53)$$

with $\check{\mathbf{M}}(n | \mathbf{b}_{1:n}) = \check{\mathbf{M}}^{(m)}(n | \mathbf{b}_{1:n-1})$ and $\check{\mathbf{M}}(n | \mathbf{b}_{1:n-1}) = \check{\mathbf{M}}^{(0)}(n | \mathbf{b}_{1:n-1})$.

Proof: Write $\check{\mathbf{M}}(n | \mathbf{b}_{1:n}) = \check{\mathbf{M}}(n | \mathbf{b}_{1:n-1}) - \Delta\check{\mathbf{M}}_m(n)$ and use Corollary 2. Recall that by definition $\check{\mathbf{M}}(n | \mathbf{b}_{1:n-1}) = \check{\mathbf{M}}^{(0)}(n | \mathbf{b}_{1:n-1})$ and $\check{\mathbf{M}}(n | \mathbf{b}_{1:n}) = \check{\mathbf{M}}^{(m)}(n | \mathbf{b}_{1:n-1})$. \blacksquare

Equation (53) is instructive in terms of understanding the MSE performance of m-IQKF. In particular, note that for $c_m = 1$, (53) coincides with the correction ECM of the KF in (10). Furthermore, as $m \rightarrow \infty$, we find $c_m \rightarrow 1$, implying that for infinite number of quantization bits we recover the clairvoyant KF. This important consistency result is summarized in the following corollary.

Corollary 4: *As the number of quantization bits $m \rightarrow \infty$, the correction step ECM at time n of the m-IQKF converges to the ECM of the clairvoyant KF provided that $\mathbf{b}_{1:n-1} = \mathbf{y}_{1:n-1}$, i.e.,*

$$\lim_{m \rightarrow \infty} \check{\mathbf{M}}^{(m)}(n | \mathbf{b}_{1:n-1}) = \check{\mathbf{M}}(n | \mathbf{y}_{1:n}). \quad (54)$$

Proof: As $m \rightarrow \infty$, we have

$$\lim_{m \rightarrow \infty} c_m = \lim_{m \rightarrow \infty} [1 - (1 - (2/\pi))^m] = 1.$$

For $c_m = 1$, $\check{\mathbf{M}}^{(m)}(n | \mathbf{b}_{1:n-1})$ [cf. (53)] and $\check{\mathbf{M}}(n | \mathbf{y}_{1:n})$ [cf. (10)] become identical for $\mathbf{b}_{1:n-1} = \mathbf{y}_{1:n-1}$, which results in (54). \blacksquare

Corollary 4 establishes that m-IQKF asymptotically (in the number of quantization bits) achieves the per correction step MSE performance of the clairvoyant KF. As demonstrated by simulations in Section V, even a small number of quantization bits ($m = 2$ or $m = 3$) renders the MSE performance of m-IQKF indistinguishable from that of the clairvoyant KF.

We remark that Corollary 2 quantifies the *per time-step* ECM reduction for the proposed filter. Because of error accumulation however, noticeable differences could emerge between the MSEs of the m-IQKF given by $\text{tr}\{\check{\mathbf{M}}(n | \mathbf{b}_{1:n})\}$ and that of the clairvoyant KF, $\text{tr}\{\check{\mathbf{M}}(n | \mathbf{y}_{1:n})\}$, as time progresses.

B. m-IQKF for Vector Observations

So far, a low-complexity scalar quantizer was employed to digitize the scalar analog-valued observations $y(n)$ at each sensor. A more general case is when sensor observations are vector-valued, $\mathbf{y}(n) \in \mathbb{R}^q$, $q > 1$ (for vector state $\mathbf{x}(n) \in \mathbb{R}^p$, $p > 1$), for which an MSE optimal estimator-quantizer would entail vector quantization of $\mathbf{y}(n)$ using an

estimation-based distortion metric [7]. Optimal state estimation based on vector quantized observations is left for future work.

In this section, an optimal bit allocation scheme for iterative scalar quantization of components of $\mathbf{y}(n)$ is introduced whose performance will be compared against the clairvoyant Kalman filter based on un-quantized $\mathbf{y}(n)$. The vector observation equation is given by $\mathbf{y}(n) = \mathbf{H}(n)\mathbf{x}(n) + \mathbf{v}(n)$ where $\mathbf{H}(n) \in \mathbb{R}^{(q \times p)}$, $\mathbf{y}(n) := [y(n, 1), \dots, y(n, q)]$, and $\mathbf{v}(n) := [v(n, 1), \dots, v(n, q)]$ with $\mathbf{C}_v(n) := E\{\mathbf{v}(n)\mathbf{v}^T(n)\}$. If $\mathbf{C}_v(n) \neq \mathbf{I}$ a noise whitening transformation of $\mathbf{y}(n)$ is performed by setting $\mathbf{y}'(n) := \mathbf{C}_v^{-1/2}(n)\mathbf{y}(n)$ resulting in

$$\begin{aligned} \mathbf{y}'(n) &= \mathbf{C}_v^{-1/2}(n)\mathbf{H}(n)\mathbf{x}(n) + \mathbf{C}_v^{-1/2}(n)\mathbf{v}(n) \\ &:= \mathbf{H}'(n)\mathbf{x}(n) + \mathbf{v}'(n) \end{aligned} \quad (55)$$

where the noise term $\mathbf{v}'(n) := \mathbf{C}_v^{-1/2}(n)\mathbf{v}(n)$ is white.

If the matrix $\mathbf{H}'(n)$ is tall (i.e., $q > p$), optimal dimensionality reduction can be performed in (55) using the QR-factorization $\mathbf{H}'(n) = \mathbf{Q}_1(n)\mathbf{R}_1(n)$, where $\mathbf{Q}_1(n) \in \mathbb{R}^{(q \times p)}$ has p orthonormal columns and $\mathbf{R}_1(n) \in \mathbb{R}^{(p \times p)}$ is upper triangular [2, p. 682]. Projection of the q -dimensional $\mathbf{y}(n)$ onto the p -dimensional space spanned by the rows of $\mathbf{Q}_1(n)$ is given by

$$\begin{aligned} \mathbf{Q}_1^T(n)\mathbf{y}'(n) &= \mathbf{Q}_1^T(n)\mathbf{H}'(n)\mathbf{x}(n) + \mathbf{Q}_1^T(n)\mathbf{v}'(n) \\ &= \mathbf{R}_1(n)\mathbf{x}(n) + \mathbf{Q}_1^T(n)\mathbf{v}'(n) \end{aligned} \quad (56)$$

where $\mathbf{Q}_1^T(n)\mathbf{H}'(n) = \mathbf{Q}_1^T(n)\mathbf{Q}_1(n)\mathbf{R}_1(n) = \mathbf{R}_1(n)$ and $\mathbf{Q}_1^T(n)E\{\mathbf{v}(n)\mathbf{v}^T(n)\}\mathbf{Q}_1(n) = \mathbf{I}$. Thus, using (56) we can henceforth assume that $\mathbf{y}(n)$ is p -dimensional with white noise, i.e., after using the correspondences $\mathbf{y}(n) \leftrightarrow \mathbf{Q}_1^T(n)\mathbf{y}'(n)$, $\mathbf{H}(n) \leftrightarrow \mathbf{Q}_1^T(n)\mathbf{H}'(n)$, and $\mathbf{v}(n) \leftrightarrow \mathbf{Q}_1^T(n)\mathbf{v}'(n)$.

Let m bits be used for quantizing the entries $\{y(n, l)\}_{l=1}^p$ of $\mathbf{y}(n) \in \mathbb{R}^p$. Clearly, there are p^m possible bit allocation choices. To reduce the complexity of a bit allocation scheme, the iterative quantizer of (43), performing sequential binary quantization, will be employed. Iterative scalar quantization and MMSE estimation entails selecting the entries of $\mathbf{y}(n)$ to be quantized and estimation by the m-IQKF algorithm of Proposition 3. The resultant MMSE is given by the trace of the first p entries of (47) i.e., $\text{tr}\{\mathbf{M}^{(i)}(n | \mathbf{b}_{1:n-1})\}$. Iterative bit allocation of the m bits leads to p choices of scalars to quantize for each of the m bits leading to $p \times m$ choices—significantly less than the exponential number of searches (p^m) needed for an optimal bit allocation. Proposition 4 summarizes the i th bit allocation for the m-IQKF of [P4]-[C6].

Proposition 4: Consider vector observations $\mathbf{y}(n) = \mathbf{H}(n)\mathbf{x}(n) + \mathbf{v}(n)$ where $E\{\mathbf{v}(n)\mathbf{v}^T(n)\} = \mathbf{I}$. The corresponding augmented-state equivalent observations are $\check{\mathbf{y}}(n) = \check{\mathbf{H}}(n)\check{\mathbf{x}}(n) + \check{\mathbf{v}}(n)$, where $\check{\mathbf{H}}(n) = [\mathbf{H}(n), \mathbf{I}] \in \mathbb{R}^{(p \times 2p)}$, $\check{\mathbf{x}}(n) = [\mathbf{x}^T(n), \mathbf{v}^T(n)]^T \in \mathbb{R}^{2p}$, and $\check{\mathbf{v}}(n) = \mathbf{0}$. Let $\check{\mathbf{h}}^T(n, l)$ denote the l th row of $\check{\mathbf{H}}(n)$. Given m bits for iterative quantization of the components of $\check{\mathbf{y}}(n)$ (i.e., $\{\check{y}(n, l)\}_{l=1}^p$) for the m-IQKF of [P4]-[C6] [cf. Section IV-A], the MMSE of estimator of $\check{\mathbf{x}}(n)$ is achieved by allocating the i th bit to the component $\check{y}(n, l^{(i)})$, where $l^{(i)}$ is given as

$$l^{(i)} = \arg \max_{l=1,2,\dots,p} \frac{\left\| \left[\check{\mathbf{M}}^{(i-1)}(n | \mathbf{b}_{1:n-1})\check{\mathbf{h}}(n, l) \right]_{1:p} \right\|_2^2}{\check{\mathbf{h}}^T(n, l)\check{\mathbf{M}}^{(i-1)}(n | \mathbf{b}_{1:n-1})\check{\mathbf{h}}(n, l)}. \quad (57)$$

Proof: From (47), the estimator MSE reduction due to i th quantization bit $b^{(i)}(n)$ is given as

$$\text{tr} \left\{ \frac{2 \left[\check{\mathbf{M}}^{(i-1)}(n | \mathbf{b}_{1:n-1})\check{\mathbf{h}}(n)\check{\mathbf{h}}^T(n)\check{\mathbf{M}}^{(i-1)}(n | \mathbf{b}_{1:n-1}) \right]_{1:p,1:p}}{\check{\mathbf{h}}^T(n)\check{\mathbf{M}}^{(i-1)}(n | \mathbf{b}_{1:n-1})\check{\mathbf{h}}(n)} \right\}$$

$$= \frac{2 \left\| \left[\check{\mathbf{M}}^{(i-1)}(n | \mathbf{b}_{1:n-1})\check{\mathbf{h}}(n) \right]_{1:p} \right\|_2^2}{\pi \check{\mathbf{h}}^T(n)\check{\mathbf{M}}^{(i-1)}(n | \mathbf{b}_{1:n-1})\check{\mathbf{h}}(n)}. \quad (58)$$

Minimizing (58) over the choices of $\check{\mathbf{h}}(n) := \check{\mathbf{h}}(n, l)$ corresponds to selecting scalar components $\{\check{y}(n, l)\}_{l=1}^p$ to be quantized as $b^{(i)}(n) = \text{sign}\{\check{y}(n, l) - \check{\mathbf{h}}^T(n, l)\check{\mathbf{x}}^{(i)}(n | \mathbf{b}_{1:n-1})\}$. The sequence of minimizations for each bit $i = 1, 2, \dots, m$ is therefore obtained by (57). ■

C. Performance Analysis of the m-IQKF

We have quantified the *per correction step* ECM reduction $\Delta \check{\mathbf{M}}_m(n)$ in the m-IQKF as a function of the number of bits m used for iteratively quantizing the scalar observations $y(n)$ in Section IV-A. We next compare the MSE performance of m-IQKF with that of the clairvoyant KF, when both prediction and correction steps are considered, by deriving the continuous-time Riccati equations for both filters.

Consider first the discrete-time algebraic Riccati equation (ARE) for the m-IQKF [P4]-[C6]. Note that regardless of the structure of $\check{\mathbf{M}}(n-1 | \mathbf{b}_{1:n-1})$, substituting for $\check{\mathbf{A}}(n)$ and $\mathbf{C}_{\check{\mathbf{u}}}(n)$ in (45) will result in

$$\check{\mathbf{M}}(n | \mathbf{b}_{1:n-1}) = \begin{pmatrix} \mathbf{M}(n | \mathbf{b}_{1:n-1}) & \mathbf{0} \\ \mathbf{0}^T & c_v(n) \end{pmatrix} \quad (59)$$

with $\mathbf{M}(n | \mathbf{b}_{1:n-1}) = \mathbf{A}(n)\mathbf{M}(n-1 | \mathbf{b}_{1:n-1})\mathbf{A}^T(n) + \mathbf{C}_{\mathbf{u}}(n)$. Equation (59) shows that the predicted ECM for the augmented-state has a block-diagonal structure.

To simplify notation let $\check{\mathbf{M}}(n+1) := \check{\mathbf{M}}(n+1 | \mathbf{b}_{1:n})$, $\check{\mathbf{M}}(n) := \check{\mathbf{M}}(n | \mathbf{b}_{1:n-1})$, $\mathbf{M}(n+1) := \mathbf{M}(n+1 | \mathbf{b}_{1:n})$, $\mathbf{M}(n) := \mathbf{M}(n | \mathbf{b}_{1:n-1})$, and substitute (53) in (45) to obtain the m-IQKF ARE for the ECM of $\check{\mathbf{x}}(n)$ as

$$\begin{aligned} \check{\mathbf{M}}(n+1) &= \check{\mathbf{A}}(n+1)\check{\mathbf{M}}(n)\check{\mathbf{A}}^T(n+1) + \mathbf{C}_{\check{\mathbf{u}}}(n+1) \\ &\quad - c_m \frac{\check{\mathbf{A}}(n+1)\check{\mathbf{M}}(n)\check{\mathbf{h}}(n)\check{\mathbf{h}}^T(n)\check{\mathbf{M}}(n)\check{\mathbf{A}}^T(n+1)}{\check{\mathbf{h}}^T(n)\check{\mathbf{M}}(n)\check{\mathbf{h}}(n)}. \end{aligned} \quad (60)$$

Substituting for $\check{\mathbf{A}}(n+1)$, $\mathbf{C}_{\check{\mathbf{u}}}(n+1)$, $\check{\mathbf{h}}(n)$ and $\check{\mathbf{M}}(n)$ in (60), and equating both sides of the upper $p \times p$ block-diagonal submatrices of the resulting expressions, yields the ARE for the ECM of $\mathbf{x}(n)$ as

$$\begin{aligned} \mathbf{M}(n+1) &= \mathbf{A}(n+1)\mathbf{M}(n)\mathbf{A}^T(n+1) + \mathbf{C}_{\mathbf{u}}(n+1) \\ &\quad - c_m \frac{\mathbf{A}(n+1)\mathbf{M}(n)\mathbf{h}(n)\mathbf{h}^T(n)\mathbf{M}(n)\mathbf{A}^T(n+1)}{\mathbf{h}^T(n)\mathbf{M}(n)\mathbf{h}(n) + c_v(n)}. \end{aligned} \quad (61)$$

Interestingly, the resulting ARE for the ECM of the m-IQKF estimate $\check{\mathbf{x}}(n+1 | \mathbf{b}_{1:n})$ [cf. (61)], becomes identical to the ARE of the clairvoyant KF ([17], Ch. 5.11), as $\lim_{m \rightarrow \infty} c_m = 1$. The implication of these relations will become clear from the continuous-time ARE for the m-IQKF given in Proposition 5, where (1) and (2) are viewed as discrete-time equivalent of a continuous-time state space model.

Proposition 5: The continuous-time ECM $\mathbf{M}_c(t) = \mathbf{M}_c(nT_s) := \lim_{T_s \rightarrow 0} \mathbf{M}(n; T_s)$ for the m-IQKF of (44)–(47) is the solution of the following differential (Riccati) equation:

$$\begin{aligned} \dot{\mathbf{M}}_c(t) &= \mathbf{A}_c(t)\mathbf{M}_c(t) + \mathbf{M}_c(t)\mathbf{A}_c^T(t) + \mathbf{C}_{\mathbf{u}}(t) \\ &\quad - \mathbf{M}_c(t)\mathbf{h}_c(t) \left[\frac{c_{v_c}(t)}{c_m} \right]^{-1} \mathbf{h}_c^T(t)\mathbf{M}_c(t). \end{aligned} \quad (62)$$

Proof: The derivation steps from (61) to (62) are the same as those followed for deriving the KF Riccati equation from the corresponding ECMs [17, pp. 259], [21]. The only difference is that the scale factor, c_m , in front of the third term on the RHS of (61) for the KF equals to 1. ■

TABLE IV
NOISE VARIANCE PENALTY FOR ITERATIVE QUANTIZATION

bits, m	1	2	3	4
$(1/c_m - 1)100\%$	57.08%	15.21%	5.04%	1.77%

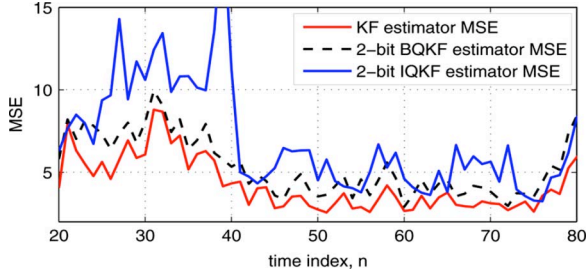


Fig. 2. Batch versus iterative quantization: Comparison of empirical estimate of the MSE, $\text{tr}\{\mathbf{M}(n | \mathbf{b}_{1:n})\}$, for 2 quantization bits.

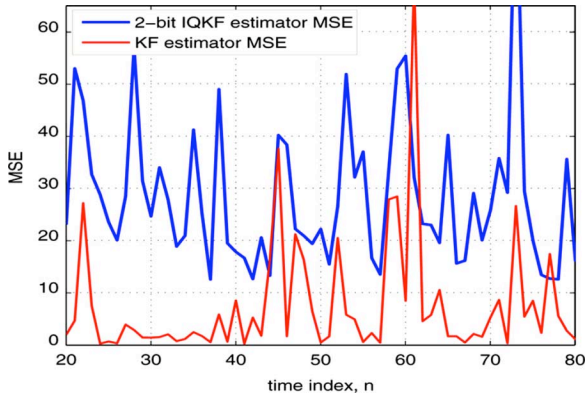


Fig. 3. Iterative quantized KF: MSE for iteratively quantized vector observations compared against the clairvoyant Kalman filter, with $\mathbf{C}_v = 20\mathbf{I}$, $\mathbf{C}_u = 10\mathbf{I}$, and $p = 4$.

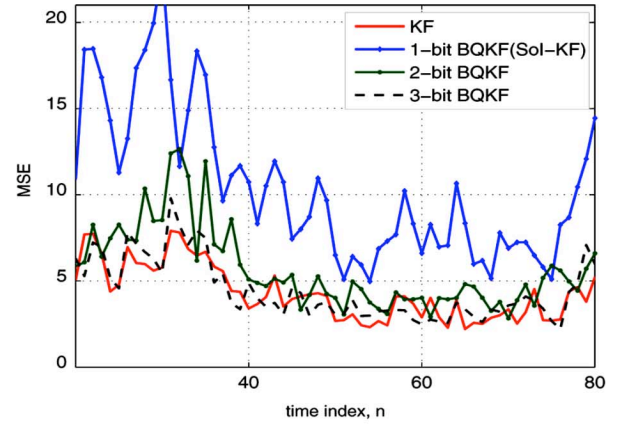
When comparing (62) to the clairvoyant KF ARE [17, pp. 259]

$$\dot{\mathbf{M}}_c^K(t) = \mathbf{A}_c(t)\mathbf{M}_c^K(t) + \mathbf{M}_c^K(t)\mathbf{A}_c^T(t) + \mathbf{C}_u(t) - \mathbf{M}_c^K(t)\mathbf{h}_c(t)[c_{v_c}(t)]^{-1}\mathbf{h}_c^T(t)\mathbf{M}_c^K(t) \quad (63)$$

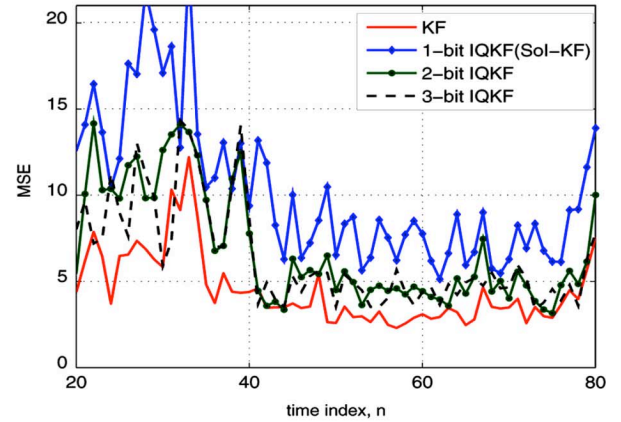
where $\mathbf{M}_c^K(t)$ denotes the continuous-time ECM of KF, it is evident that the variance of the continuous-time observation noise of the m -IQKF is amplified by $1/c_m$ compared to that of the clairvoyant KF. This is the price paid for using quantized observations, $b(n)$, instead of the analog-amplitude ones, $y(n)$. Note that $2/\pi \leq c_m = 1 - (1 - 2/\pi)^m \leq 1$. Table IV shows the percentage observation noise variance increase versus the number of quantization bits, m . Surprisingly, even with only 4-bit quantization, the observation noise variance increase is less than 2% of the analog-amplitude observations variance. In the next section, simulations for the two quantizer-estimator approaches (batch and iterative) are provided in order to corroborate the analytical statements and validate model consistency.

V. SIMULATIONS

Target tracking in \mathbb{R}^2 is simulated here with the target position $\mathbf{s}(n) := [s_1(n), s_2(n)]^T$ and velocity $\mathbf{w}(n) := [w_1(n), w_2(n)]^T$ forming a state vector $\mathbf{x}(n) := [\mathbf{s}(n)^T, \mathbf{w}(n)^T]^T$ with state equation



(a)



(b)

Fig. 4. (a) Batch quantized KF, (b) Iteratively quantized KF: Empirical estimate of the MSE, $\text{tr}\{\mathbf{M}(n | \mathbf{b}_{1:n})\}$, found by averaging Monte Carlo runs for 1–3 quantization bits. Empirical MSE for clairvoyant KF is included for comparison.

$$\begin{pmatrix} \mathbf{s}(n) \\ \mathbf{w}(n) \end{pmatrix} = \begin{pmatrix} 1 & 0 & T_s & 0 \\ 0 & 1 & 0 & T_s \\ 0 & 0 & 1 & 0 \\ 0 & 0 & 0 & 1 \end{pmatrix} \begin{pmatrix} \mathbf{s}(n-1) \\ \mathbf{w}(n-1) \end{pmatrix} + \begin{pmatrix} T_s^2/2 & 0 \\ 0 & T_s^2/2 \\ T_s & 0 \\ 0 & T_s \end{pmatrix} \mathbf{u}(n) \quad (64)$$

where $T_s = 1$ denotes sampling period. The model describes a constant-velocity tracking set-up [1, pp. 82], where the acceleration term is captured by the noise term $\mathbf{u}(n)$. Uniformly deployed sensors take noisy Euclidean distance measurements of the target. Sensor \mathcal{S}_k , located at position \mathbf{x}^k measures

$$y_k(n) = \|\mathbf{x}(n) - \mathbf{x}^k\| + v(n). \quad (65)$$

Linearizing (65) about a generic state prediction $\hat{\mathbf{x}}(n | n-1)$ in similar fashion to the extended Kalman filter (E)KF, we obtain

$$y_k(n) \approx \mathbf{h}_k^T(n)\mathbf{x}(n) + y_k^0(n) + v(n) \quad (66)$$

where $\mathbf{h}_k(n) = \frac{\hat{\mathbf{x}}(n | n-1) - \mathbf{x}^k}{\|\hat{\mathbf{x}}(n | n-1) - \mathbf{x}^k\|}$ and $y_k^0(n)$ is a function of $\hat{\mathbf{x}}(n | n-1)$ and \mathbf{x}^k ; The linearized observations (66) together with (64) are amenable to the IQKF and BQKF algorithms of Sections III and IV.

WSN data corresponding to $K = 100$ sensors are simulated. All plots generated illustrate the evolution of the MSEs, obtained from the trace of the respective ECMs, against the time index n . Figs. 4(a), 5(a), and (b) are for the batch quantized KF whereas Figs. 4(b), 6(a), and (b) are for the iteratively quantized

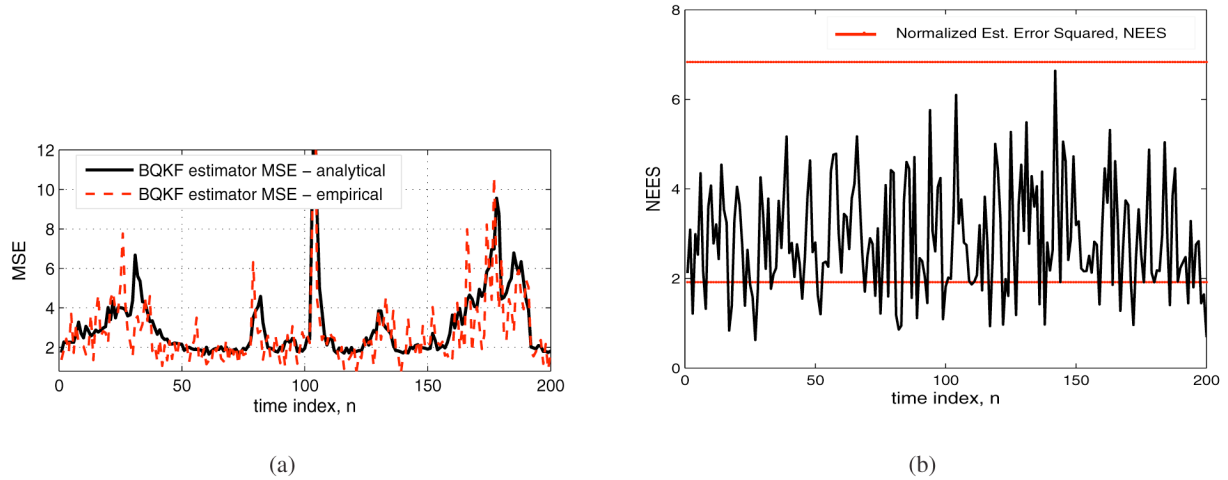


Fig. 5. (a) Batch quantized KF: Consistency test comparing empirical MSE (from Monte Carlo runs) and analytical MSE. (b) Batch quantized KF: Consistency test using normalized estimation error squared (NEES) $[\mathbf{x}(n) - \hat{\mathbf{x}}(n | \mathbf{b}_{1:n})]^T \mathbf{M}(n | \mathbf{b}_{1:n})^{-1} [\mathbf{x}(n) - \hat{\mathbf{x}}(n | \mathbf{b}_{1:n})]$, compared with the 95% confidence region using 2 quantization bits.

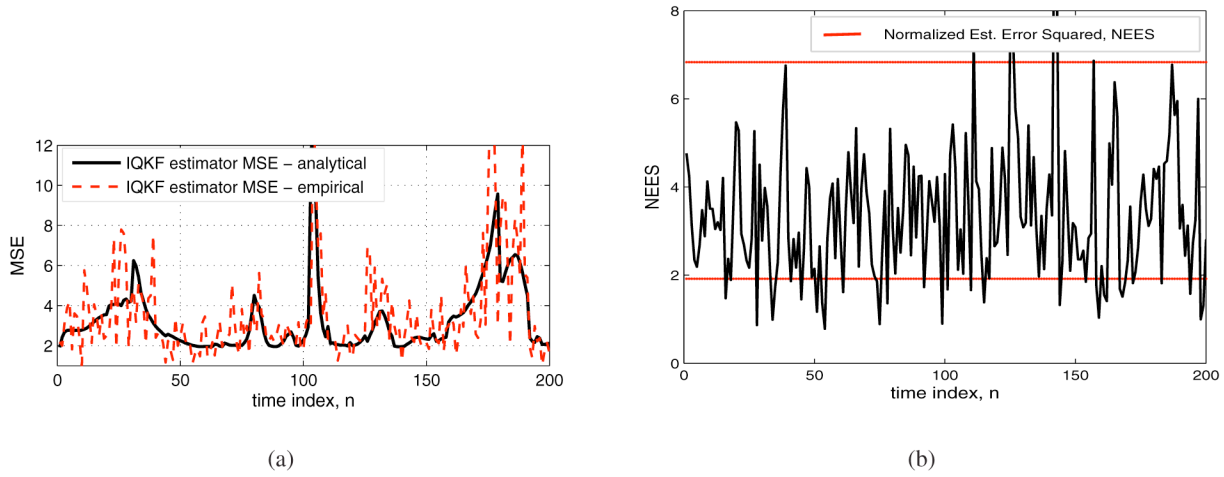


Fig. 6. (a) Iteratively quantized KF: Consistency test comparing empirical MSE (from Monte Carlo runs) and analytical MSE. (b) Iteratively quantized KF: Consistency test using normalized estimation error squared (NEES) $[\mathbf{x}(n) - \hat{\mathbf{x}}(n | \mathbf{b}_{1:n})]^T \mathbf{M}(n | \mathbf{b}_{1:n})^{-1} [\mathbf{x}(n) - \hat{\mathbf{x}}(n | \mathbf{b}_{1:n})]$, compared with the 95% confidence region using 2 quantization bits.

KF. The MSE for a linear state space model with vector measurements based on the bit allocation of Section IV-B is shown in Fig. 3 for 2-bits IQKF.

The simulation results of Fig. 4(a) depicts the BQKF MSE given by $\text{tr}\{\mathbf{M}(n | \mathbf{b}_{1:n})\}$. The simulations are performed for 1, 2, and 3 bits and the respective MSEs are compared with the MSE of the clairvoyant KF. The plots demonstrate the MSE improvement offered by 2 quantization bits compared to the 1-bit BQKF case. It is evident that quantization to more than 2 bits offers little MSE improvement. Model consistency checks comparing the empirically obtained MSEs with analytical MSEs are depicted in Fig. 5(a). Note that the analytical MSE is obtained from the trace of the ECM $\mathbf{M}(n | \mathbf{b}_{1:n}) := \mathbb{E}\{[\mathbf{x}(n) - \hat{\mathbf{x}}(n | \mathbf{b}_{1:n})][\mathbf{x}(n) - \hat{\mathbf{x}}(n | \mathbf{b}_{1:n})]^T | \mathbf{b}_{1:n}\}$ defined in Section III. The empirical MSE is the sample estimator of $\text{tr}\{\mathbf{M}(n | \mathbf{b}_{1:n})\}$ obtained as a sample average of the squared estimation errors. The consistency check reveals that the empirical and analytical MSEs are nearly identical.

Fig. 5(b) shows alternative model consistency tests for the BQKF using the normalized estimation error squared (NEES) tests of [1, Ch. 5.4]. NEES $r(n) := [\mathbf{x}(n) - \hat{\mathbf{x}}(n | \mathbf{b}_{1:n})]^T [\mathbf{M}(n | \mathbf{b}_{1:n})]^{-1} [\mathbf{x}(n) - \hat{\mathbf{x}}(n | \mathbf{b}_{1:n})]$

is postulated to have a χ^2 pdf with p degrees of freedom (since the p -dimensional $\tilde{\mathbf{x}}(n) := \mathbf{x}(n) - \hat{\mathbf{x}}(n | \mathbf{b}_{1:n})$ is assumed zero-mean Gaussian with covariance $\mathbf{M}(n | \mathbf{b}_{1:n})$ if the estimator is consistent with the model). Under the hypothesis that the estimator is consistent, L realizations of the NEES statistics $\{r_i(n)\}_{i=1}^L$ each χ^2 distributed with p degrees of freedom, lead to a χ^2 distribution with Lp degrees of freedom. This is checked by running Monte Carlo simulations and computing the sample average NEES $\hat{r}(n) := (1/L) \sum_{i=1}^L r_i(n)$ and then defining an acceptance (confidence) region (for the consistent hypothesis). If $l \leq \hat{r}(n) \leq u$, then the estimator is consistent; lower and upper bounds l and u are obtained from $\Pr\{\hat{r}_n \in [l, u]\} = 1 - \alpha$, where $1 - \alpha$ is the probability of acceptance region. Using $L = 50$ realizations, state space of $p = 4$ dimensions, and $\alpha = 0.05$ (i.e., 95% region), we observed that about 72% of 200 time samples simulated are within the 95% acceptance region.

In Fig. 4(b), the MSE of the IQKF is compared with the MSE of the clairvoyant KF. Once again we observe a substantial MSE reduction when going from 1 to 2 quantization bits and very little performance gain for higher number of bits as was the case for BQKF. With 2 quantization bits the MSE performance is vir-

tually coincident with that of the clairvoyant KF as was postulated by the analytical values in Table III whereby $c_2 = 86.8\%$.

In Figs. 6(a) and (b), model consistency of the IQKF estimator is checked. The IQKF algorithm's analytical MSE is compared with the empirical MSE evaluated through Monte Carlo runs depicted in Fig. 6(a). The analytical and the empirical MSEs match well. The alternative NEES consistency test for the iteratively quantized KF is presented in Fig. 6(b), where $p = 4$, 200 time samples, and $\alpha = 0.05$ are used. About 80% time samples lie inside the 95% acceptance region.

MSE comparison between 2-BQKF and 2-IQKF is depicted in Fig. 2. The respective MSEs are very close. However, the BQKF exhibits slightly smaller MSE which happens because the iterative approach uses the Gaussian approximation on $p[\mathbf{x}(n) | \mathbf{b}_{1:n-1}, \mathbf{b}^{(1:i)}(n)]$ a number of times (m) per time-step (Proposition 3), whereas the batch approach invokes this approximation only once per time-step (Proposition 1). Fig. 3 demonstrates that the low complexity iterative scalar quantization has potential for application in vector observation cases as well.

VI. CONCLUDING REMARKS

Recursive state estimators based on quantized observations were considered. Multi-bit quantization was done by either an iterative binary quantizer or a single-shot batch quantization of the measurement innovations to a block of bits. Motivated by the need to find quantifiable trade-offs between estimation performance and number of quantization bits for decentralized estimation, it was shown that quantization using 2 to 3 bits improves the performance of Kalman-like algorithms to virtually coincide with the optimal state estimator (Kalman filter), with only minimal increase in computation. Numerical simulations were used to compare the filter true covariances with analytical ones, to check model consistency issues, as well as for performance comparison of the two quantization-estimation approaches. The mean-square error performances for both batch and iteratively quantized estimators were found to be close to the clairvoyant KF for a tracking example involving a Gauss-Markov model.

Future directions include studying decentralized estimation based on quantized vector observations, and incorporation of particle filters for the correction step in order to avoid the Gaussian approximation of the prior pdf. Robustness issues of the algorithms to noisy intersensor channels is also worth pursuing.²

APPENDIX A

PROOF OF PROPOSITION 1: DERIVATION OF BQKF

The proof will rely on a result known as iterated conditional expectation [6, pp. 37] which asserts that: Given random variables $\mathbf{x} \in \mathbb{R}^p$, $y \in \mathcal{R}_i \subset \mathbb{R}$, where \mathcal{R}_i and \mathbb{R} are Borel fields and a function $g(\cdot)$ defined on \mathbb{R}^p , it holds that

$$E\{g(\mathbf{x}) | y \in \mathcal{R}_i\} = E\{E\{g(\mathbf{x}) | Y\} | y \in \mathcal{R}_i\} \quad (67)$$

where Y denotes a random variable in \mathbb{R} and y is its realization. The proof of (67) is given by

$$E\{E\{g(\mathbf{x}) | Y\} | y \in \mathcal{R}_i\}$$

²The views and conclusions contained in this document are those of the authors and should not be interpreted as representing the official policies, either expressed or implied, of the Army Research Laboratory or the U.S. Government.

$$= \int_{\mathbb{R}} \left[\int_{\mathbb{R}^p} g(\mathbf{x}) p(\mathbf{x} | Y = \zeta) d\mathbf{x} \right] p(\zeta | y \in \mathcal{R}_i) d\zeta \\ = \int_{\mathcal{R}_i} \left[\int_{\mathbb{R}^p} g(\mathbf{x}) p(\mathbf{x} | Y = \zeta) d\mathbf{x} \right] \frac{p(\zeta)}{\Pr\{y \in \mathcal{R}_i\}} d\zeta \quad (68)$$

$$= \int_{\mathbb{R}^p} g(\mathbf{x}) \left[\int_{\mathcal{R}_i} \frac{p(\mathbf{x}, \zeta)}{\Pr\{y \in \mathcal{R}_i\}} d\zeta \right] d\mathbf{x} \\ = \int_{\mathbb{R}^p} g(\mathbf{x}) p(\mathbf{x} | y \in \mathcal{R}_i) d\mathbf{x} = E\{g(\mathbf{x}) | y \in \mathcal{R}_i\} \quad (69)$$

where in (68) and (69) we have used the conditional pdfs

$$p(\zeta | y \in \mathcal{R}_i) = \begin{cases} \frac{p(\zeta)}{\Pr\{y \in \mathcal{R}_i\}}, & \text{if } \zeta \in \mathcal{R}_i \\ 0, & \text{otherwise} \end{cases} \\ p(\mathbf{x} | y \in \mathcal{R}_i) = \int_{\mathcal{R}_i} \frac{p(\mathbf{x}, \zeta)}{\Pr\{y \in \mathcal{R}_i\}} d\zeta. \quad \blacksquare$$

Subsequent derivations will use substitutions $\mathbf{x} \leftrightarrow \mathbf{x}(n); Y \leftrightarrow [\mathbf{b}_{1:n-1}, \tilde{y}(n)]$; and $y \leftrightarrow [\mathbf{b}_{1:n-1}, \tilde{y}(n) \in \mathcal{R}_i]$. To derive $\hat{\mathbf{x}}(n | \mathbf{b}_{1:n}) = E\{\mathbf{x}(n) | \mathbf{b}_{1:n-1}, b(n)\}$ in (20) for $b(n) = i$ where $\mathcal{R}_i = [\tau_i(n), \tau_{i+1}(n))$ (i.e., $\tilde{y}(n) \in \mathcal{R}_i$), let $g(\mathbf{x}(n)) = \mathbf{x}(n)$ which, from (67), leads to

$$E\{\mathbf{x}(n) | \mathbf{b}_{1:n-1}, b(n) = i\} \\ = E\{E\{\mathbf{x}(n) | \mathbf{b}_{1:n-1}, \tilde{y}(n)\} | \mathbf{b}_{1:n-1}, b(n) = i\}. \quad (70)$$

We will first evaluate the inner expectation in (70) for which the pdf $p[\mathbf{x}(n) | \mathbf{b}_{1:n-1}, \tilde{y}(n)]$ is needed. If $p[\mathbf{x}(n) | \mathbf{b}_{1:n-1}] = \mathcal{N}[\mathbf{x}(n); \hat{\mathbf{x}}(n | \mathbf{b}_{1:n-1}), \mathbf{M}(n | \mathbf{b}_{1:n-1})]$, where $\hat{\mathbf{x}}(n | \mathbf{b}_{1:n-1}) := E\{\mathbf{x}(n) | \mathbf{b}_{1:n-1}\}$ and $\mathbf{M}(n | \mathbf{b}_{1:n-1}) = E\{[\mathbf{x}(n) - \hat{\mathbf{x}}(n | \mathbf{b}_{1:n-1})][\mathbf{x}(n) - \hat{\mathbf{x}}(n | \mathbf{b}_{1:n-1})]^T\}$ with $\tilde{\mathbf{x}}(n) := \mathbf{x}(n) - \hat{\mathbf{x}}(n | \mathbf{b}_{1:n-1})$ and $\tilde{y}(n) := \mathbf{h}^T(n)\tilde{\mathbf{x}}(n) + v(n)$, then $p[\tilde{y}(n) | \mathbf{b}_{1:n-1}] = \mathcal{N}[\tilde{y}(n); 0, \sigma_{y_n}^2]$, where $\sigma_{y_n}^2 = \mathbf{h}^T(n)\mathbf{M}(n | \mathbf{b}_{1:n-1})\mathbf{h}(n) + c_v(n)$. Since $\tilde{y}(n) = \mathbf{h}^T(n)\tilde{\mathbf{x}}(n) + v(n)$, the joint conditional pdf of $\mathbf{x}(n), \tilde{y}(n)$ is Gaussian, i.e.,

$$p[\mathbf{x}(n), \tilde{y}(n) | \mathbf{b}_{1:n-1}] = \mathcal{N}\left[\mathbf{x}(n), \tilde{y}(n); \begin{pmatrix} \hat{\mathbf{x}}(n | \mathbf{b}_{1:n-1}) \\ 0 \end{pmatrix}, \begin{pmatrix} \mathbf{M}(n | \mathbf{b}_{1:n-1}) & \mathbf{M}(n | \mathbf{b}_{1:n-1})\mathbf{h}(n) \\ \mathbf{h}^T(n)\mathbf{M}(n | \mathbf{b}_{1:n-1}) & \sigma_{y_n}^2 \end{pmatrix}\right] \quad (71)$$

and thus the inner expectation becomes

$$\hat{\mathbf{x}}^c(n | \mathbf{b}_{1:n}) := E\{\mathbf{x}(n) | \mathbf{b}_{1:n-1}, \tilde{y}(n)\} \\ = E\{\mathbf{x}(n) | \mathbf{b}_{1:n-1}\} + E\{\tilde{\mathbf{x}}(n) | \mathbf{b}_{1:n-1}, \tilde{y}(n)\} \\ = \hat{\mathbf{x}}(n | \mathbf{b}_{1:n-1}) + \mathbf{k}^c(n)\tilde{y}(n) \quad (72)$$

where

$$\mathbf{k}^c(n) := \frac{\mathbf{M}(n | \mathbf{b}_{1:n-1})\mathbf{h}(n)}{\sigma_{y_n}^2} \quad (73)$$

since it is the conditional mean of jointly Gaussian random variables [cf. (71)] (similar to the KF in a Gauss-Markov model [12, pp. 472]). The outer expectation in (70) follows from (72) as $\hat{\mathbf{x}}(n | \mathbf{b}_{1:n}) = E\{\hat{\mathbf{x}}^c(n | \mathbf{b}_{1:n}) | \mathbf{b}_{1:n-1}, b(n) = i\}$

$= \hat{\mathbf{x}}(n | \mathbf{b}_{1:n-1}) + \mathbf{k}^c(n)E\{\tilde{y}(n) | \mathbf{b}_{1:n-1}, b(n) = i\}$. (74) The pdf $p[\tilde{y}(n) | \mathbf{b}_{1:n-1}, b(n) = i] = p[\tilde{y}(n) | \mathbf{b}_{1:n-1}, \tilde{y}(n) \in \mathcal{R}_i]$ is obtained from Bayes' theorem as

$$p[\tilde{y}(n) | \mathbf{b}_{1:n-1}, b(n) = i] \\ = \begin{cases} \frac{p[\tilde{y}(n) | \mathbf{b}_{1:n-1}]}{\Pr\{\tilde{y}(n) \in \mathcal{R}_i | \mathbf{b}_{1:n-1}\}}, & \text{if } \tilde{y}(n) \in \mathcal{R}_i \\ 0, & \text{otherwise} \end{cases} \quad (75)$$

and thus the expectation in the second term of (74) becomes $E\{\tilde{y}(n) | \mathbf{b}_{1:n-1}, b(n) = i\}$

$$= \frac{\int_{\mathcal{R}_i} \tilde{y}(n) p[\tilde{y}(n) | \mathbf{b}_{1:n-1}] d\tilde{y}(n)}{\Pr\{\tilde{y}(n) \in \mathcal{R}_i | \mathbf{b}_{1:n-1}\}}. \quad (76)$$

Since $p[\tilde{y}(n) | \mathbf{b}_{1:n-1}] = \mathcal{N}[\tilde{y}(n); 0, \sigma_{y_n}^2]$, and $\{\tilde{y}(n) \in \mathcal{R}_i\} \equiv \{b(n) = i\}$, (76) becomes

$$\begin{aligned} & \mathbb{E}\{\tilde{y}(n) | \mathbf{b}_{1:n-1}, b(n) = i\} \\ &= \frac{\int_{\tau_i(n)}^{\tau_{i+1}(n)} \tilde{y}(n) \mathcal{N}[\tilde{y}(n); 0, \sigma_{y_n}^2] d\tilde{y}(n)}{\Pr\{\tau_i(n) \leq \tilde{y}(n) < \tau_{i+1}(n) | \mathbf{b}_{1:n-1}\}} \\ &= \frac{\sigma_{y_n}}{\sqrt{2\pi}} \frac{\exp\left[-\frac{\tau_i^2(n)}{2\sigma_{y_n}^2}\right] - \exp\left[-\frac{\tau_{i+1}^2(n)}{2\sigma_{y_n}^2}\right]}{Q\left[\frac{\tau_i(n)}{\sigma_{y_n}}\right] - Q\left[\frac{\tau_{i+1}(n)}{\sigma_{y_n}}\right]} \\ &= \frac{\sigma_{y_n}}{\sqrt{2\pi}} \frac{\exp[-\Delta_i^2(n)/2] - \exp[-\Delta_{i+1}^2(n)/2]}{Q[\Delta_i(n)] - Q[\Delta_{i+1}(n)]} \\ &:= \sigma_{y_n} \alpha_i(n). \end{aligned} \quad (77)$$

where $\Delta_i(n) := \tau_i(n)/\sigma_{y_n}$ and the last equality follows from the definition of $\alpha_i(n)$ in (18). Substituting (77) in (74), $\mathbf{k}^c(n)$ from (73) and $\sigma_{y_n}^2 := \mathbf{h}^T(n)\mathbf{M}(n | \mathbf{b}_{1:n-1})\mathbf{h}(n) + c_v(n)$, we obtain [cf. (20)]

$$\hat{\mathbf{x}}(n | \mathbf{b}_{1:n}) = \hat{\mathbf{x}}(n | \mathbf{b}_{1:n-1}) + \alpha_i(n) \frac{\mathbf{M}(n | \mathbf{b}_{1:n-1})\mathbf{h}(n)}{\sigma_{y_n}}. \quad (78)$$

We next derive (21) using $\mathbf{M}(n | \mathbf{b}_{1:n}) := \mathbb{E}\{[\mathbf{x}(n) - \hat{\mathbf{x}}(n | \mathbf{b}_{1:n})][\mathbf{x}(n) - \hat{\mathbf{x}}(n | \mathbf{b}_{1:n})]^T | \mathbf{b}_{1:n}\}$. It should be noted that given $\mathbf{b}_{1:n}$, as in most nonlinear filtering, see e.g., [9], the conditional ECM defined above is different from the unconditional ECM $\bar{\mathbf{M}}(n | \mathbf{b}_{1:n}) := \mathbb{E}\{[\mathbf{x}(n) - \hat{\mathbf{x}}(n | \mathbf{b}_{1:n})][\mathbf{x}(n) - \hat{\mathbf{x}}(n | \mathbf{b}_{1:n})]^T\}$. In contrast, for the Gauss-Markov model in the clairvoyant KF [P2]-[C2] the ECM $\mathbf{M}(n | \mathbf{y}_{1:n})$ is independent of $\mathbf{y}_{1:n}$, i.e., $\mathbf{M}(n | \mathbf{y}_{1:n}) = \mathbf{M}(n | \mathbf{y}_{1:n})$. Derivation of $\mathbf{M}(n | \mathbf{b}_{1:n})$ uses again the iterated conditional expectation in (67). We first write $\mathbf{x}(n) - \hat{\mathbf{x}}(n | \mathbf{b}_{1:n})$ using (72) and (74) as follows:

$$\begin{aligned} & \mathbf{x}(n) - \hat{\mathbf{x}}(n | \mathbf{b}_{1:n}) \\ &= \mathbf{x}(n) - \hat{\mathbf{x}}^c(n | \mathbf{b}_{1:n}) + \hat{\mathbf{x}}^c(n | \mathbf{b}_{1:n}) - \hat{\mathbf{x}}(n | \mathbf{b}_{1:n}) \\ &= \mathbf{x}(n) - \hat{\mathbf{x}}^c(n | \mathbf{b}_{1:n}) \\ &\quad + \mathbf{k}^c(n)[\tilde{y}(n) - \mathbb{E}\{\tilde{y}(n) | \mathbf{b}_{1:n-1}, b(n) = i\}]. \end{aligned} \quad (79)$$

With $g(\mathbf{x}(n)) = [\mathbf{x}(n) - \hat{\mathbf{x}}(n | \mathbf{b}_{1:n})][\mathbf{x}(n) - \hat{\mathbf{x}}(n | \mathbf{b}_{1:n})]^T$ in (67), the ECM $\mathbf{M}(n | \mathbf{b}_{1:n})$ can be written as

$$\begin{aligned} \mathbf{M}(n | \mathbf{b}_{1:n}) &= \mathbb{E}\{g(\mathbf{x}(n)) | \mathbf{b}_{1:n-1}, b(n) = i\} \\ &= \mathbb{E}\{\mathbb{E}\{g(\mathbf{x}(n)) | \mathbf{b}_{1:n-1}, \tilde{y}(n)\} | \mathbf{b}_{1:n-1}, b(n) = i\}. \end{aligned} \quad (80)$$

Considering first the inner expectation, we obtain upon substituting from (79)

$$\begin{aligned} & \mathbb{E}\{g(\mathbf{x}(n)) | \mathbf{b}_{1:n-1}, \tilde{y}(n)\} = \mathbb{E}\{[\mathbf{x}(n) - \hat{\mathbf{x}}^c(n | \mathbf{b}_{1:n})][\mathbf{x}(n) \\ &\quad - \hat{\mathbf{x}}^c(n | \mathbf{b}_{1:n})]^T | \mathbf{b}_{1:n-1}, \tilde{y}(n)\} \\ &\quad + \mathbf{k}^c(n)[\tilde{y}(n) - \mathbb{E}\{\tilde{y}(n) | \mathbf{b}_{1:n-1}, b(n) = 1\}] \\ &\quad \times [\tilde{y}(n) - \mathbb{E}\{\tilde{y}(n) | \mathbf{b}_{1:n-1}, b(n)\}]^T \mathbf{k}^{cT}(n). \end{aligned} \quad (81)$$

This expression follows since both $\tilde{y}(n)$ and $\mathbb{E}\{\tilde{y}(n) | \mathbf{b}_{1:n-1}, b(n)\}$ are deterministic functions of the variables $\mathbf{b}_{1:n-1}, \tilde{y}(n)$ and $\mathbb{E}\{[\mathbf{x}(n) - \hat{\mathbf{x}}^c(n | \mathbf{b}_{1:n}) | \mathbf{b}_{1:n-1}, \tilde{y}(n)]\} = \mathbb{E}\{\mathbf{x}(n) | \mathbf{b}_{1:n-1}, \tilde{y}(n)\} - \hat{\mathbf{x}}^c(n | \mathbf{b}_{1:n}) = \hat{\mathbf{x}}^c(n | \mathbf{b}_{1:n}) - \hat{\mathbf{x}}^c(n | \mathbf{b}_{1:n}) = \mathbf{0}$. Since $\hat{\mathbf{x}}^c(n | \mathbf{b}_{1:n}) = \mathbb{E}\{\mathbf{x}(n) | \mathbf{b}_{1:n-1}, \tilde{y}(n)\}$, we observe that the first term of (81) is the covariance of $p[\mathbf{x}(n) | \mathbf{b}_{1:n-1}, \tilde{y}(n)]$, which from $p[\mathbf{x}(n), \tilde{y}(n) | \mathbf{b}_{1:n-1}]$ in (71) is given by

$$\begin{aligned} & \mathbf{M}^c(n | \mathbf{b}_{1:n}) := \mathbb{E}\{[\mathbf{x}(n) - \hat{\mathbf{x}}^c(n | \mathbf{b}_{1:n})][\mathbf{x}(n) \\ &\quad - \hat{\mathbf{x}}^c(n | \mathbf{b}_{1:n})]^T | \mathbf{b}_{1:n-1}, \tilde{y}(n)\} \\ &= \mathbf{M}(n | \mathbf{b}_{1:n-1}) - \mathbf{k}^c(n)\mathbf{h}^T(n)\mathbf{M}(n | \mathbf{b}_{1:n-1}). \end{aligned} \quad (82)$$

Next, we pursue the outer expectation in (80) using (82) to obtain

$$\begin{aligned} & \mathbf{M}(n | \mathbf{b}_{1:n}) = \mathbf{M}^c(n | \mathbf{b}_{1:n}) + \mathbf{k}^c(n) \\ &\quad \times \mathbb{E}\{[\tilde{y}(n) - \mathbb{E}\{\tilde{y}(n) | \mathbf{b}_{1:n}\}] \\ &\quad \times [\tilde{y}(n) - \mathbb{E}\{\tilde{y}(n) | \mathbf{b}_{1:n}\}]^T | \mathbf{b}_{1:n}\} \mathbf{k}^{cT}(n) \\ &= \mathbf{M}^c(n | \mathbf{b}_{1:n}) + \mathbf{k}^c(n) \text{var}\{\tilde{y}(n) | \mathbf{b}_{1:n}\} \mathbf{k}^{cT}(n). \end{aligned} \quad (83)$$

The conditional variance term in (83) can be expressed using the pdf in (75) as

$$\begin{aligned} & \text{var}\{\tilde{y}(n) | \mathbf{b}_{1:n-1}, b(n) = i\} \\ &= \mathbb{E}\{\tilde{y}^2(n) | \mathbf{b}_{1:n-1}, b(n) = i\} \\ &\quad - \mathbb{E}^2\{\tilde{y}(n) | \mathbf{b}_{1:n-1}, b(n) = i\} \\ &= \frac{\int_{\tau_i(n)}^{\tau_{i+1}(n)} \tilde{y}^2(n) p[\tilde{y}(n) | \mathbf{b}_{1:n-1}] d\tilde{y}(n)}{\Pr\{\tau_i(n) \leq \tilde{y}(n) < \tau_{i+1}(n) | \mathbf{b}_{1:n-1}\}} \\ &\quad - \mathbb{E}^2\{\tilde{y}(n) | \mathbf{b}_{1:n-1}, b(n) = i\}. \end{aligned} \quad (84)$$

Using integration by parts, the numerator of the first term of (84) is

$$\begin{aligned} & \int_{\tau_i(n)}^{\tau_{i+1}(n)} \tilde{y}^2(n) \mathcal{N}[\tilde{y}(n); 0, \sigma_{y_n}^2] d\tilde{y}(n) \\ &= -\frac{\sigma_{y_n}}{\sqrt{2\pi}} \left[\tilde{y}(n) e^{-\frac{\tilde{y}^2(n)}{2\sigma_{y_n}^2}} \right]_{\tau_i(n)}^{\tau_{i+1}(n)} + \frac{\sigma_{y_n}}{\sqrt{2\pi}} \int_{\tau_i(n)}^{\tau_{i+1}(n)} e^{-\frac{\tilde{y}^2(n)}{2\sigma_{y_n}^2}} d\tilde{y}(n) \\ &= \frac{\sigma_{y_n}^2}{\sqrt{2\pi}} \left[\frac{\tau_i(n)}{\sigma_{y_n}} \exp\left(-\frac{\tau_i^2(n)}{2\sigma_{y_n}^2}\right) - \frac{\tau_{i+1}(n)}{\sigma_{y_n}} \exp\left(-\frac{\tau_{i+1}^2(n)}{2\sigma_{y_n}^2}\right) \right] \\ &\quad + \sigma_{y_n}^2 \left[Q\left(\frac{\tau_i(n)}{\sigma_{y_n}}\right) - Q\left(\frac{\tau_{i+1}(n)}{\sigma_{y_n}}\right) \right] \\ &= \frac{\sigma_{y_n}^2}{\sqrt{2\pi}} \left[\Delta_i(n) \exp\left(-\frac{\Delta_i^2(n)}{2}\right) - \Delta_{i+1}(n) \exp\left(-\frac{\Delta_{i+1}^2(n)}{2}\right) \right] \\ &\quad + \sigma_{y_n}^2 [Q(\Delta_i(n)) - Q(\Delta_{i+1}(n))] \end{aligned}$$

where $\Delta_i(n) := \tau_i(n)/\sigma_{y_n}$. The second term of (84) is the square of (77), i.e., $\sigma_{y_n}^2 \alpha_i^2(n)$. Since $\Pr\{\tau_i(n) \leq \tilde{y}(n) < \tau_{i+1}(n) | \mathbf{b}_{1:n-1}\} = Q(\Delta_i(n)) - Q(\Delta_{i+1}(n))$, it follows that (84) becomes

$$\begin{aligned} & \text{var}\{\tilde{y}(n) | \mathbf{b}_{1:n-1}, b(n) = i\} \\ &= \frac{\sigma_{y_n}^2}{\sqrt{2\pi}} \frac{\Delta_i(n) \exp(-\frac{1}{2}\Delta_i^2(n)) - \Delta_{i+1}(n) \exp(-\frac{1}{2}\Delta_{i+1}^2(n))}{Q(\Delta_i(n)) - Q(\Delta_{i+1}(n))} \\ &\quad + \sigma_{y_n}^2 - \sigma_{y_n}^2 \alpha_i^2(n) := \sigma_{y_n}^2 [1 - \beta_i(n)] \end{aligned} \quad (85)$$

where the last equality follows from the definition of $\beta_i(n)$ in (19). Substituting $\mathbf{M}^c(n | \mathbf{b}_{1:n})$ from (82) and the variance in (85) into (83), we obtain

$$\begin{aligned} & \mathbf{M}(n | \mathbf{b}_{1:n}) = \mathbf{M}(n | \mathbf{b}_{1:n-1}) - \mathbf{k}^c(n)\mathbf{h}^T(n)\mathbf{M}(n | \mathbf{b}_{1:n-1}) \\ &\quad + \mathbf{k}^c(n)\sigma_{y_n}^2 [1 - \beta_i(n)] \mathbf{k}^{cT}(n). \end{aligned} \quad (86)$$

Expanding $\mathbf{k}^{cT}(n)$ based on (73) we have $\mathbf{k}^c(n)\sigma_{y_n}^2 \mathbf{k}^{cT}(n) = \mathbf{k}^c(n)\mathbf{h}^T(n)\mathbf{M}(n | \mathbf{b}_{1:n-1})$ which when substituted into (86), simplifies $\mathbf{M}(n | \mathbf{b}_{1:n})$ to

$$\begin{aligned} & \mathbf{M}(n | \mathbf{b}_{1:n}) \\ &= \mathbf{M}(n | \mathbf{b}_{1:n-1}) - \beta_i(n)\mathbf{k}^c(n)\mathbf{h}^T(n)\mathbf{M}(n | \mathbf{b}_{1:n-1}) \\ &= \mathbf{M}(n | \mathbf{b}_{1:n-1}) - \beta_i(n) \\ &\quad \times \frac{\mathbf{M}(n | \mathbf{b}_{1:n-1})\mathbf{h}(n)\mathbf{h}^T(n)\mathbf{M}(n | \mathbf{b}_{1:n-1})}{\sigma_{y_n}^2} \end{aligned} \quad (87)$$

which is the ECM in (21). \blacksquare

APPENDIX B

PROOF OF PROPOSITION 3: DERIVATION OF IQKF

We first prove the predictor step [P4] of (44) and (45) using the state equation (39). Taking expectation with respect to $p[\check{\mathbf{x}}(n) | \mathbf{b}_{1:n-1}]$, we obtain (44) as

$$\begin{aligned}\hat{\check{\mathbf{x}}}(n | \mathbf{b}_{1:n-1}) &:= E\{\check{\mathbf{x}}(n) | \mathbf{b}_{1:n-1}\} \\ &= \check{\mathbf{A}}(n) E\{\check{\mathbf{x}}(n-1) | \mathbf{b}_{1:n-1}\} + E\{\check{\mathbf{u}}(n) | \mathbf{b}_{1:n-1}\} \\ &= \check{\mathbf{A}}(n) \hat{\check{\mathbf{x}}}(n-1 | \mathbf{b}_{1:n-1})\end{aligned}$$

where since $\mathbf{b}_{1:n-1}$ are quantized versions of $\{\check{y}(1), \check{y}(2), \dots, \check{y}(n-1)\}$, it follows that $E\{\check{\mathbf{u}}(n) | \mathbf{b}_{1:n-1}\} = E\{\check{\mathbf{u}}(n)\} = \mathbf{0}$; and also [cf. Proposition 3], $\hat{\check{\mathbf{x}}}(n | \mathbf{b}_{1:n-1}) := E\{\check{\mathbf{x}}(n) | \mathbf{b}_{1:n-1}\}$ and $\hat{\check{\mathbf{x}}}(n-1 | \mathbf{b}_{1:n-1}) := E\{\check{\mathbf{x}}(n-1) | \mathbf{b}_{1:n-1}\}$.

To find an expression for $\check{\mathbf{M}}(n | \mathbf{b}_{1:n-1}) := E\{[\hat{\check{\mathbf{x}}}(n | \mathbf{b}_{1:n-1}) - \check{\mathbf{x}}(n)][\hat{\check{\mathbf{x}}}(n | \mathbf{b}_{1:n-1}) - \check{\mathbf{x}}(n)]^T\}$ we use $\hat{\check{\mathbf{x}}}(n | \mathbf{b}_{1:n-1}) - \check{\mathbf{x}}(n) = \check{\mathbf{A}}(n)[\hat{\check{\mathbf{x}}}(n-1 | \mathbf{b}_{1:n-1}) - \check{\mathbf{x}}(n-1)] - \check{\mathbf{u}}(n)$ from (39). We thus obtain (45) as

$$\begin{aligned}\check{\mathbf{M}}(n | \mathbf{b}_{1:n-1}) &= \check{\mathbf{A}}(n) E\{[\hat{\check{\mathbf{x}}}(n-1 | \mathbf{b}_{1:n-1}) - \check{\mathbf{x}}(n-1)] \\ &\quad \times [\hat{\check{\mathbf{x}}}(n-1 | \mathbf{b}_{1:n-1}) - \check{\mathbf{x}}(n-1)]^T\} \check{\mathbf{A}}^T(n) \\ &\quad + E\{\check{\mathbf{u}}(n) \check{\mathbf{u}}^T(n)\} \\ &= \check{\mathbf{A}}(n) \check{\mathbf{M}}(n-1 | \mathbf{b}_{1:n-1}) \check{\mathbf{A}}^T(n) + \mathbf{C}_{\check{\mathbf{u}}}(n)\end{aligned}$$

where $E\{[\hat{\check{\mathbf{x}}}(n-1 | \mathbf{b}_{1:n-1}) - \check{\mathbf{x}}(n-1)] \check{\mathbf{u}}^T(n)\} = \mathbf{0}$, since $\check{\mathbf{u}}(n)$ is uncorrelated with $\check{\mathbf{x}}(n-1)$ and $\mathbf{b}_{1:n-1}$.

We next derive the corrector step [C6] based on the approach used for deriving the corrector step of the more general batch quantized KF in Appendix A. The proof details the i th iterative step in (46)–(47) using $p[\check{\mathbf{x}}(n) | \mathbf{b}_{1:n-1}, \mathbf{b}^{(1:i-1)}(n)] = \mathcal{N}[\check{\mathbf{x}}(n); \hat{\check{\mathbf{x}}}^{(i-1)}(n | \mathbf{b}_{1:n-1}), \check{\mathbf{M}}^{(i-1)}(n | \mathbf{b}_{1:n-1})]$ and the binary quantizer in (43). The quantization intervals are defined as $\mathcal{R}_j := [\tau_j(n), \tau_{j+1}(n))$, $j \in \{1, 2\}$ where $\tau_1(n) = -\infty$, $\tau_2(n) = 0$, and $\tau_3(n) = +\infty$, similar to the quantizer of BQKF detailed in Section III.

Let $\check{\check{\mathbf{x}}}(n) := \check{\mathbf{x}}(n) - \hat{\check{\mathbf{x}}}^{(i-1)}(n | \mathbf{b}_{1:n-1})$, $\check{y}(n) := \check{y}(n) - \check{\mathbf{h}}^T(n) \hat{\check{\mathbf{x}}}^{(i-1)}(n | \mathbf{b}_{1:n-1}) = \check{\mathbf{h}}^T(n) \check{\check{\mathbf{x}}}(n) + \check{v}(n)$, where $\check{y}(n)$ is defined in (40). Since $\check{\mathbf{x}}(n)$ and $\check{v}(n)$ conditioned on $[\mathbf{b}_{1:n-1}, \mathbf{b}^{(1:i-1)}(n)]$ are Gaussian and independent, by using $\sigma_{y_n}^2 := \check{\mathbf{h}}^T(n) \check{\mathbf{M}}^{(i-1)}(n | \mathbf{b}_{1:n-1}) \check{\mathbf{h}}(n) + c_v(n)$, we have

$$\begin{aligned}p[\check{\mathbf{x}}(n), \check{y}(n) | \mathbf{b}_{1:n-1}, \mathbf{b}^{(1:i-1)}(n)] \\ = \mathcal{N}\left[\check{\mathbf{x}}(n), \check{y}(n); \begin{pmatrix} \hat{\check{\mathbf{x}}}^{(i-1)}(n | \mathbf{b}_{1:n-1}) \\ 0 \end{pmatrix}, \right. \\ \left. \begin{pmatrix} \check{\mathbf{M}}^{(i-1)}(n | \mathbf{b}_{1:n-1}) & \check{\mathbf{M}}^{(i-1)}(n | \mathbf{b}_{1:n-1}) \check{\mathbf{h}}(n) \\ \check{\mathbf{h}}^T(n) \check{\mathbf{M}}^{(i-1)}(n | \mathbf{b}_{1:n-1}) & \sigma_{y_n}^2 \end{pmatrix}\right].\end{aligned}\quad (88)$$

From (88), it is clear that if $\check{y}(n) \in \mathcal{R}_j$ for $j \in \{1, 2\}$, then $\hat{\check{\mathbf{x}}}^{(i)}(n | \mathbf{b}_{1:n-1})$ [cf. (46)] and $\check{\mathbf{M}}^{(i)}(n | \mathbf{b}_{1:n-1})$ [cf. (47)] are the conditional mean and conditional covariance of $p[\check{\mathbf{x}}(n) | \mathbf{b}_{1:n-1}, \mathbf{b}^{(1:i-1)}(n), \check{y}(n) \in \mathcal{R}_j]$ and can be found using the iterated conditional means in the same way as for the BQKF in Appendix A. In fact, for $N = 2$ (binary quantizer) with $\tau_1(n) = -\infty$, $\tau_2(n) = 0$, $\tau_3(n) = +\infty$, and $\Delta_j(n) = \tau_j(n)/\sigma_{y_n}$, we have $\Delta_1(n) = -\infty$, $\Delta_2(n) = 0$ and $\Delta_3(n) = +\infty$.

Equation (78) then simplifies to

$$\begin{aligned}\hat{\check{\mathbf{x}}}^{(i)}(n | \mathbf{b}_{1:n-1}) &= \hat{\check{\mathbf{x}}}^{(i-1)}(n | \mathbf{b}_{1:n-1}) \\ &\quad + \sqrt{\frac{2}{\pi}} \frac{\check{\mathbf{M}}^{(i-1)}(n | \mathbf{b}_{1:n-1}) \check{\mathbf{h}}(n)}{\sigma_{y_n}} b^{(i)}(n)\end{aligned}$$

where [cf. (18)] $\frac{\exp[-\Delta_j^2(n)/2] - \exp[-\Delta_{j+1}^2(n)/2]}{Q[\Delta_j(n)] - Q[\Delta_{j+1}(n)]}$ equals $-2(+2)$ if $j = 1$ ($j = 2$). This is the estimator in (46), since the noise variance $c_v(n) = 0$ in the augmented state formulation detailed in Section IV-A.

Likewise for the ECM $\check{\mathbf{M}}^{(i)}(n | \mathbf{b}_{1:n-1})$ —see (87) and its derivation—we can use this binary quantizer (in place of the batch quantizer in Appendix A) and the resulting $\{\Delta_j(n)\}_{j=1}^3$ to show that $\beta_j(n) = 2/\pi$ [cf. (19)] which leads to the conditional ECM

$$\begin{aligned}\check{\mathbf{M}}^{(i)}(n | \mathbf{b}_{1:n-1}) &= \check{\mathbf{M}}^{(i-1)}(n | \mathbf{b}_{1:n-1}) \\ &\quad - \frac{2}{\pi} \frac{\check{\mathbf{M}}^{(i-1)}(n | \mathbf{b}_{1:n-1}) \check{\mathbf{h}}(n) \check{\mathbf{h}}^T(n) \check{\mathbf{M}}^{(i-1)}(n | \mathbf{b}_{1:n-1})}{\check{\mathbf{h}}^T(n) \check{\mathbf{M}}^{(i-1)}(n | \mathbf{b}_{1:n-1}) \check{\mathbf{h}}(n)}\end{aligned}$$

as given in (47). ■

APPENDIX C

PROOF THAT $\Delta(n) = 0$ MINIMIZES $\bar{\beta}(n)$ IN (31)

Upon defining $x := \Delta(n)$ in (31) and $g(x) = e^{x^2} Q(x) Q(-x)$, it follows readily that

$$\arg \max_{\Delta(n) \in \mathbb{R}} \bar{\beta}(n) = \arg \min_{x \in \mathbb{R}} g(x). \quad (89)$$

Note that $g(x)$ is symmetric about $x = 0$, i.e., $g(x) = g(-x)$. To show that $x = 0$ minimizes $g(x)$ and consequently $\Delta(n) = 0$ maximizes $\bar{\beta}(n)$, we will prove that $g(x)$ is convex and symmetric. To this end, we use the following lemma:

Lemma 2: *If a function $f(x)$ is convex and symmetric about $x = 0$, then $f(0)$ is a minimum of $f(x)$.*

Proof: Letting $f(x)$ be convex and symmetric, we have that $f(\lambda x_1 + (1-\lambda)x_2) \leq \lambda f(x_1) + (1-\lambda)f(x_2)$, $\forall x_1, x_2 \in \mathbb{R}$, and $0 \leq \lambda \leq 1$. Also, by symmetry of $f(x)$, we have $f(x) = f(-x)$, $\forall x \in \mathbb{R}$. Setting $x_1 = x$, $x_2 = -x$, and $\lambda = 1/2$, we obtain $f(0) \leq f(x)$, $\forall x \in \mathbb{R}$. ■

We next prove that $g(x)$ is convex. From [22, pp. 85, 88], $Q(x) = (1/\pi) \int_0^{\pi/2} e^{-(x^2/2 \sin^2 \theta)} d\theta$, and $Q^2(x) = (1/\pi) \int_0^{\pi/4} e^{-(x^2/2 \sin^2 \theta)} d\theta$ from which

$$\begin{aligned}g(x) &= e^{x^2} Q(x) [1 - Q(x)] \\ &= e^{x^2} [Q(x) - Q^2(x)] \\ &= \frac{1}{\pi} \int_{\pi/4}^{\pi/2} e^{x^2(1 - \frac{1}{2 \sin^2 \theta})} d\theta.\end{aligned}$$

Since $\forall \theta \in [\pi/4, \pi/2)$, we have $1 - (1/2 \sin^2 \theta) \geq 0$, hence $e^{x^2(1 - (1/2 \sin^2 \theta))}$ is convex w.r.t. x for $\theta \in [\pi/4, \pi/2)$. From [2, pp. 79], integration (or sum) of convex functions preserves convexity. Thus, $g(x)$ is convex and symmetric, and by Lemma 2, $x = 0$ minimizes $g(x)$. From (89), $\Delta(n) = 0$ maximizes $\bar{\beta}(n)$ in (31). ■

REFERENCES

- [1] Y. Bar-Shalom and X. Li, *Estimation and Tracking: Principles, Techniques, and Software*. Norwood, MA: Artech House, 1993.
- [2] S. Boyd and L. Vandenberghe, *Convex Optimization*. Cambridge, U.K.: Cambridge Univ. Press, 2004.
- [3] C. Y. Chong and S. Kumar, "Sensor networks: Evolution, opportunities, and challenges," *Proc. IEEE*, vol. 91, pp. 27–41, Aug. 2003.
- [4] D. Culler, D. Estrin, and M. Srivastava, "Overview of sensor networks," *Computer*, vol. 37, no. 8, pp. 41–49, Aug. 2004.
- [5] P. Djuric, J. Kotecha, J. Zhang, Y. Huang, T. Ghirmai, M. Bugallo, and J. Miguez, "Particle filtering," *IEEE Signal Process. Mag.*, vol. 20, pp. 19–38, Sep. 2003.

- [6] J. Doob, *Stochastic Processes*. New York: Wiley, 1953.
- [7] R. M. Gray, "Quantization in task-driven sensing and distributed processing," in *Proc. Int. Conf. Acoustics, Speech, Signal Processing*, Toulouse, France, May 14–19, 2006, vol. 5, pp. V-1049–V-1052.
- [8] V. Gupta, T. Chung, B. Hassibi, and R. M. Murray, "On a stochastic sensor selection algorithm with applications in sensor scheduling and dynamic sensor coverage," *Automatica*, vol. 42, pp. 251–260, Feb. 2006.
- [9] K. Ito and K. Xiong, "Gaussian filters for nonlinear filtering problems," *IEEE Trans. Autom. Control*, vol. 45, pp. 910–927, May 2000.
- [10] A. Jadbabaie, J. Lin, and A. Morse, "Coordination of groups of mobile autonomous agents using nearest neighbor rules," *IEEE Trans. Autom. Control*, vol. 48, pp. 988–1001, Jun. 2003.
- [11] S. Julier and J. Uhlmann, "Unscented filtering and nonlinear estimation," *Proc. IEEE*, vol. 92, pp. 401–422, Mar. 2004.
- [12] S. M. Kay, *Fundamentals of Statistical Signal Processing—Estimation Theory*. Englewood Cliffs, NJ: Prentice-Hall, 1993.
- [13] J. Kotecha and P. Djuric, "Gaussian particle filtering," *IEEE Trans. Signal Process.*, vol. 51, no. 10, pp. 2602–2612, Oct. 2003.
- [14] S. Lloyd, "Least squares quantization in PCM," *IEEE Trans. Inf. Theory*, vol. 28, no. 2, pp. 129–137, Mar. 1982.
- [15] A. Mainwaring, D. Culler, J. Polastre, R. Szewczyk, and J. Anderson, "Wireless sensor networks for habitat monitoring," in *Proc. 1st ACM Intl. Workshop Wireless Sensor Networks Applications*, Atlanta, GA, 2002, vol. 3, pp. 88–97.
- [16] J. Max, "Quantizing for minimum distortion," *IEEE Trans. Inf. Theory*, vol. 6, pp. 7–12, Mar. 1960.
- [17] P. S. Maybeck, *Stochastic Models, Estimation and Control—Vol. 1*. New York: Academic, 1979.
- [18] A. I. Mourikis and S. I. Roumeliotis, "Optimal sensing strategies for mobile robot formations: Resource constrained localization," in *Proc. Robotics: Sci. Syst. Conf.*, Cambridge, MA, 2005, pp. 281–288.
- [19] H. Papadopoulos, G. Wornell, and A. Oppenheim, "Sequential signal encoding from noisy measurements using quantizers with dynamic bias control," *IEEE Trans. Inf. Theory*, vol. 47, no. 3, pp. 978–1002, Mar. 2001.
- [20] A. Ribeiro and G. B. Giannakis, "Bandwidth-constrained distributed estimation for wireless sensor networks, Part II: Unknown pdf," *IEEE Trans. Signal Process.*, vol. 54, no. 3, pp. 1131–1143, Mar. 2006.
- [21] A. Ribeiro, G. B. Giannakis, and S. I. Roumeliotis, "SOI-KF: Distributed Kalman filtering with low-cost communications using the sign of innovations," *IEEE Trans. Signal Process.*, vol. 54, no. 12, pp. 4782–4795, Dec. 2006.
- [22] M. K. Simon and M. S. Alouini, *Digital Communications Over Fading Channels*. New York: Wiley-Interscience, 2000.



Eric J. Msechu (S'07) received the B.Sc. degree in electrical engineering from the University of Dar es Salaam, Tanzania, in 1999 and the M.Sc. in communications technology from the University of Ulm, Germany, in 2004. Since August 2004, he has been working towards the Ph.D. degree in electrical engineering at the Department of Electrical and Computer Engineering, University of Minnesota, Minneapolis.

From 1999 to 2001, he worked as a Cellular Systems Engineer for Millicom International Cellular, Tanzania. His current research interests are in statistical signal processing for distributed ad hoc wireless sensor networks.



Stergios I. Roumeliotis (M'00) received the Diploma degree in electrical engineering from the National Technical University of Athens, Greece, in 1995 and the M.S. and Ph.D. degrees in electrical engineering from the University of Southern California, Los Angeles, in 1997 and 2000, respectively.

From 2000 to 2002, he was a Postdoctoral Fellow at the California Institute of Technology, Pasadena. Since 2002, he has been an Assistant Professor in the Department of Computer Science and Engineering at the University of Minnesota, Minneapolis. His research interests include inertial navigation of aerial and ground autonomous vehicles, fault detection and identification, and sensor networks. Recently, his research has focused on distributed estimation under communication and processing constraints and active sensing for reconfigurable networks of mobile sensors.

Dr. Roumeliotis is the recipient of the NSF CAREER award (2006) and the McKnight Land-Grant Professorship award (2006–2008), and he is the corecipient of the One NASA Peer award (2006), and the One NASA Center Best award (2006). Publications he has coauthored have received the Robotics Society of Japan Best Paper Award (2007), the ICASSP Best Student Paper Award (2006), and the NASA Tech Briefs Award (2004). He is currently serving as Associate Editor for the IEEE TRANSACTIONS ON ROBOTICS.

Dr. Roumeliotis is the recipient of the NSF CAREER award (2006) and the McKnight Land-Grant Professorship award (2006–2008), and he is the corecipient of the One NASA Peer award (2006), and the One NASA Center Best award (2006). Publications he has coauthored have received the Robotics Society of Japan Best Paper Award (2007), the ICASSP Best Student Paper Award (2006), and the NASA Tech Briefs Award (2004). He is currently serving as Associate Editor for the IEEE TRANSACTIONS ON ROBOTICS.



Alejandro Ribeiro (M'07) received the B.Sc. degree in electrical engineering from Universidad de la Republica Oriental del Uruguay, Montevideo, Uruguay, in 1998 and the M.Sc. and Ph.D. degrees in electrical engineering from the University of Minnesota, Minneapolis, in 2005 and 2006, respectively.

From 1998 to 2003, he was a Member of the Technical Staff at Bellsouth Montevideo. He is currently a Research Associate in the Department of Electrical and Computer Engineering, University of Minnesota.

His research interests lie in the areas of communication theory, signal processing, and networking. His current research focuses on wireless cooperative communications, random access, wireless ad hoc and sensor networks, and distributed signal processing.

Dr. Ribeiro is a Fulbright Scholar.



Georgios B. Giannakis (F'97) received the Diploma degree in electrical engineering from the National Technical University of Athens, Greece, in 1981. From 1982 to 1986, he was with the University of Southern California (USC), Los Angeles, where he received the M.Sc. degree in electrical engineering in 1983, the M.Sc. degree in mathematics in 1986, and the Ph.D. degree in electrical engineering in 1986.

Since 1999, he has been a Professor with the Electrical and Computer Engineering Department at the University of Minnesota, Minneapolis, where he is

now the Director of the Digital Technology Center and holds an ADC Chair in Wireless Telecommunications. His general interests span the areas of communications, networking, and statistical signal processing—subjects on which he has published more than 275 journal papers, 450 conference papers, two edited books and two upcoming research monographs on *Space-Time Coding for Broadband Wireless Communications* (Wiley, 2007) and *Ultra-Wideband Wireless Communications* (Cambridge Press, 2009). Current research focuses on diversity techniques, complex-field and space-time coding, multicarrier, cooperative wireless communications, cognitive radios, cross-layer designs, mobile ad hoc networks, and wireless sensor networks.

Dr. Giannakis is the (co-)recipient of six paper awards from the IEEE Signal Processing (SP) and Communications Societies, including the G. Marconi Prize Paper Award in Wireless Communications. He also received Technical Achievement Awards from the SP Society (2000), from EURASIP (2005), a Young Faculty Teaching Award, and the G. W. Taylor Award for Distinguished Research from the University of Minnesota. He has served the IEEE in a number of posts.